Discovery of broad-spectrum bacterial polyamine detoxification inhibitors as potential antivirulence agents and antibiotic adjuvants

Peri B. Moulding[1], Ronald S. Flannagan[2], Jonas Wong[3,4,5,6,7], Ahmed M. Soliman[1,8], Wael Elhenawy[3,4,5,6,7], David E. Heinrichs[2], and Omar M. El-Halfawy[1,9*]

[1] Department of Chemistry and Biochemistry, Faculty of Science, University of Regina, Regina, SK, S4S 0A2, Canada

[2] Department of Microbiology and Immunology, University of Western Ontario, London, Ontario, Canada

[3] Department of Medical Microbiology & Immunology, Faculty of Medicine & Dentistry, University of Alberta, Canada.

[4] Li Ka Shing Institute of Virology, Canada.

[5] Women and Children's Health Research Institute, Edmonton, Alberta, Canada.

[6] Antimicrobial Resistance, One Health Consortium - Edmonton, AB, Canada.

[7] Striving for Pandemic Preparedness - The Alberta Research Consortium - Edmonton, AB, Canada.

[8] Department of Microbiology and Immunology, Faculty of Pharmacy, Kafrelsheikh University, Kafr El-Sheikh 33516, Egypt

[9] Department of Microbiology and Immunology, Faculty of Pharmacy, Alexandria University, Alexandria, 21521, Egypt

[*] Correspondence: omar.el-halfawy@uregina.ca (O.M.E.)

Running title: Broad-spectrum polyamine detoxification inhibitors

Abstract

The alarming rise in antimicrobial resistance reinforces an urgent need for new antimicrobial strategies. Chemicals at infection sites, such as polyamines, often influence microbial virulence and antibiotic response. Polyamines are cationic small molecules overproduced by the host during infection, modulating immune responses—the ability of several pathogens to detoxify polyamines correlated with hypervirulence. We sought to uncover inhibitors of polyamine detoxification through a high-throughput whole-cell screen against the community-acquired methicillin-resistant *Staphylococcus aureus* USA300, identifying the polyamine analog OES2-0017. This inhibitor synergized with polyamines at the low micromolar range, inhibiting a polyamine detoxification spermine/spermidine acetyltransferase SSAT (SpeG) and another previously uncharacterized *S. aureus* SSAT (denoted $PaiA_{Sa}$ herein). OES2-0017 showed growth-inhibitory effects at higher concentrations, perturbing the bacterial membrane with no detectable effects against eukaryotic membranes at the same concentration range. OES2-0017 showed similar broad-spectrum activities against various Gram-positive and Gram-negative pathogens. OES2-0017 abolished the polyamine-mediated resistance to antibiotics, including vancomycin, in MRSA USA300, phenocopying the Δ*speG* mutant and suggesting its potential utility as an antibiotic adjuvant. OES2-0017 eradicated SpeG-expressing *Salmonella* Typhimurium inside murine macrophages, suggesting its potential as an antivirulence agent. Small-scale structure-activity relationship, eukaryotic toxicity, and enzymatic inhibition against the human SSAT (SAT1) assays identified analogs with higher bacterial enzyme specificity and no toxicity at the antimicrobial range. Our screen also uncovered additional inhibitors, including the catechol derivative isoproterenol (OES1-1087), showing a similar mode of action and activity as OES2-0017 but with lower potency. This study provides novel antimicrobial compounds with broad-spectrum activity and a novel mode of action for multidrug-resistant priority pathogens.

52 **Introduction**

53 Bacteria have developed resistance to all currently available antibiotics posing a
54 large public health risk. The spread of antimicrobial resistance (AMR) has exacerbated the
55 threat of bacterial infections, with 1.27 million deaths directly attributed to bacterial AMR in
56 2019 alone [1]. *Staphylococcus aureus* is a leading cause of hospital and community-
57 acquired infections, resulting in considerable morbidity and mortality rates [2]. *S. aureus* can
58 cause multiple infections, including skin and soft tissue infections (SSTI), infective
59 endocarditis, osteomyelitis, prosthetic-device infections, community-acquired pneumonia,
60 and other systemic infections [3]. Some strains of *S. aureus* have developed resistance to β-
61 lactam antibiotics, coined methicillin-resistant *Staphylococcus aureus* (MRSA). MRSA
62 strains have spread rapidly, and in 2019 alone, it was estimated that more than 100,000
63 deaths were directly attributable to MRSA infections worldwide [1]. Notably, the MRSA strain
64 USA300 has become the most common infection-causing *S. aureus* strain in Canada and
65 the USA [4,5].

66 While we continue to lose clinically useful antibiotics due to the rise of AMR, the
67 discovery and development of antimicrobials with novel chemical structures or cellular
68 targets has drastically slowed [6,7]. One of the potential reasons for the antibiotic discovery
69 void is that antimicrobial discovery efforts traditionally relied on antimicrobial susceptibility
70 testing (AST) conditions that use culture media such as Mueller-Hinton broth (MHB) [8].
71 These test conditions do not accurately reflect those at the infection site, including the
72 chemicals bacteria may encounter within the host. There is an expansive array of molecules
73 produced by the host, resident microbiota, and the infecting pathogen at the infection site,
74 which may influence microbial virulence and antibiotic responses [9,10]. Such chemical-
75 mediated effects might alter the treatment outcomes and may offer new targets for
76 antimicrobial intervention. One prominent class of compounds is polyamines, which are
77 biogenic small cationic amines, such as the diamine putrescine, triamine spermidine, and
78 tetramine spermine, required for normal cell functioning in most living organisms [11].
79 Polyamines are overproduced by the host in response to infection [12-14], and can be found at
80 millimolar concentrations in eukaryotes [15,16], where they have immunomodulatory roles [17,18].

81 Most bacteria produce polyamines endogenously, with *S. aureus* being one of few
82 exceptions that neither produce spermine or spermidine nor require them for homeostasis
83 [19-21]. For polyamine producers, polyamine levels are tightly regulated to maintain the level
84 required for homeostasis, balancing uptake and biosynthesis with detoxification and efflux

85 to prevent toxicity resulting from high and low polyamine cellular content [11,16]. On the
86 contrary, most *S. aureus* strains, being polyamine non-producers, are typically more
87 susceptible to these compounds; however, USA300 is resistant to exogenous spermine and
88 spermidine [19]. The virulence and prevalence of USA300 have been partially attributed to the
89 acquisition of the arginine catabolic mobile element (ACME) [14,22,23]. The ACME was
90 horizontally transferred to *S. aureus* from *Staphylococcus epidermidis*, and encodes SpeG,
91 a member of the GCN5-related *N*-acetyltransferase (GNAT) family [23]. SpeG is a
92 spermine/spermidine *N*-acetyltransferase (SSAT) that acetylates spermine and spermidine
93 rendering them less toxic to the cell, resulting in the observed resistance to exogenous
94 polyamines [14,19,20,23]. The ACME also encodes the arginine-deaminase (*arc*) system which
95 converts arginine to ornithine while producing ATP and ammonia, allowing USA300 to
96 withstand acidic environments, such as those found on the skin [14]. The host then converts
97 ornithine produced via the ACME-Arc system to polyamines as shown in a murine SSTI
98 model [14]. Therefore, by carrying *speG,* USA300 can resist the excessive host polyamine
99 production, increasing its virulence. Additionally, exogenous polyamines increase biofilm
100 formation, an effect lost in a Δ*speG* mutant [23].
101 Polyamine detoxification via SSAT homologs contributed to virulence in other
102 bacterial species. For example, SpeG is required for the survival of *Salmonella enterica*
103 serovar Typhimurium in macrophages [24] and the overexpression of PmvE in *Enterococcus*
104 *faecalis* increases virulence in a *Galleria mellonella* infection model [25]. Polyamines are also
105 known to alter bacterial susceptibility to antibiotics [26-30] and to influence virulence
106 phenotypes such as biofilm formation [31-33], intracellular growth [34], colonization [35], and
107 resistance to reactive oxygen species [36]. Given the correlation of the ability of pathogens to
108 detoxify polyamines with their hypervirulence and the potential for polyamine-mediated
109 alterations to antibiotic susceptibility at the site of infection, inhibiting bacterial polyamine
110 detoxification appears as an attractive strategy to reduce virulence and prevent polyamine-
111 mediated antibiotic resistance. Indeed, new treatment strategies to combat the spread of
112 AMR are desperately needed, and antivirulence agents and antibiotic adjuvants have been
113 suggested as potential therapeutic options. Antivirulence agents target processes
114 dispensable for bacterial viability but that the pathogen uses to cause infection; therefore,
115 by targeting these processes the host immune system can more easily clear the infection [37].
116 Antibiotic adjuvants are compounds that potentiate the activity of existing antibiotics,

117 restoring their effect against resistant bacteria or improving their efficacy against intrinsically
118 resistant organisms [38].
119 Here, we set out to identify inhibitors of bacterial polyamine detoxification
120 mechanisms through a cell-based high throughput screen against *S. aureus* USA300, as it
121 lacks *de novo* polyamine biosynthesis. We discovered the polyamine analog OES2-0017,
122 which showed potent synergy with polyamines (a phenotype lost in SSAT mutants) and
123 growth-inhibitory effects at the low micromolar range against various Gram-positive and
124 Gram-negative pathogens. We revealed a dual mode of action of OES2-0017, where low
125 concentrations inhibited SpeG and other polyamine detoxification enzymes, and higher
126 concentrations perturbed the bacterial membrane in *S. aureus*. Eukaryotic cell membranes
127 were not impacted at the same concentration range, as observed in a hemolysis assay. The
128 inhibitor eradicated SpeG-expressing *S.* Typhimurium inside murine macrophages,
129 suggesting its potential as an antivirulence agent. OES2-0017, at the low polyamine-
130 synergistic concentrations, abolished the polyamine-mediated resistance of MRSA USA300
131 to vancomycin and other antibiotics, suggesting its potential utility as an antibiotic adjuvant.
132 We also uncovered previously uncharacterized alternative polyamine detoxification
133 mechanisms in *S. aureus* that OES2-0017 inhibited. Our screen also uncovered additional
134 inhibitors, including the catechol derivative, isoproterenol, OES1-1087, showing similar
135 mode of action and activity as OES2-0017 but with lower potency. Together, this study
136 describes novel antimicrobial compounds with broad-spectrum activity and potential
137 antivirulence and antibiotic adjuvant applications.
138

139 **Results and Discussion**

140 **A high-throughput chemical screen identifies potential polyamine**
141 **detoxification inhibitors.** To identify inhibitors of polyamine detoxification mechanisms, we
142 undertook two screens against *S. aureus* USA300. In an unbiased approach, we screened
143 a library of 2560 small molecules (Spectrum collection, MicroSource Discovery Systems,
144 Inc.), comprised of previously approved drugs and natural product derivatives, at 20 μM in
145 the presence of ¼th the minimum inhibitory concentration (MIC) of spermine against
146 USA300. In parallel, we took a rationale-based approach by assembling a collection of 83
147 polyamine analogs with at least 60% structural similarity to substrates and products of
148 polyamine biosynthesis and detoxification enzymes in bacteria, reasoning that such analogs

149 have a higher probability of interacting with, and potentially inhibiting, the polyamine-related
150 enzymes of interest. Notably, several polyamine biosynthesis inhibitors are analogous to
151 natural polyamines or substrates of their biosynthetic enzymes [39-41], which supports this
152 rationale-based approach. We screened the polyamine analog library at 20 μM (similar to
153 the Spectrum collection screen) in the presence of spermine at ¼th the MIC. The screen
154 was performed with the hypothesis that a compound inhibiting polyamine detoxification
155 would exhibit synergy with spermine. Combined, the screens resulted in 187 primary hits
156 showing at least 80% growth inhibition. We then excluded known antimicrobials in the
157 Spectrum collection yielding 129 hits (Figure 1 A and B). We tested these hits in follow-up
158 dose-response assays in the presence and absence of a single spermine concentration
159 (Supplementary Fig. 1); only 8 compounds showed a reduction in MIC in the presence of
160 spermine (Figure 1A). We then tested these eight compounds in checkerboard assays with
161 spermine; six compounds, OES1-1087, OES1-0507, OES1-1639, OES1-1238, OES2-0052,
162 and OES2-0017, showed synergy with spermine (Figure 1C-H). Synergy was determined by
163 calculating the fractional inhibitory concentration index (FICI), with an FICI value ≤ 0.5
164 defined as a synergistic interaction. OES1-1087 exhibited the strongest synergistic
165 interaction with spermine with an FICI value of 0.15 ± 0.03 followed by OES1-0507 ($0.28 \pm$
166 0.07), OES2-0017 (0.33 ± 0.06), OES1-1639 (0.42 ± 0.06), OES1-1238 (0.46 ± 0.12), and
167 finally OES2-0052 (0.50 ± 0) (Figure 1 C-H). OES1-0507, OES1-1087, and OES1-1639 are
168 benzenediols, OES1-1238 is an acridine, and OES2-0052 and OES2-0017 are amines. In
169 addition to synergizing with polyamines, the six hits exhibited growth inhibitory effects
170 against USA300 with OES2-0017 being the most potent at an MIC of 20 μM (Figure 1C-H).
171 Of note, we prioritized OES2-0017 and OES1-1087 (isoproterenol) for further
172 characterization based on their relative potencies (spermine synergy at FICI<0.35) and as
173 representatives of different chemical classes (polyamine and catechols, respectively). We
174 confirmed the structures of the two prioritized compounds by NMR (Supplementary Fig.2).

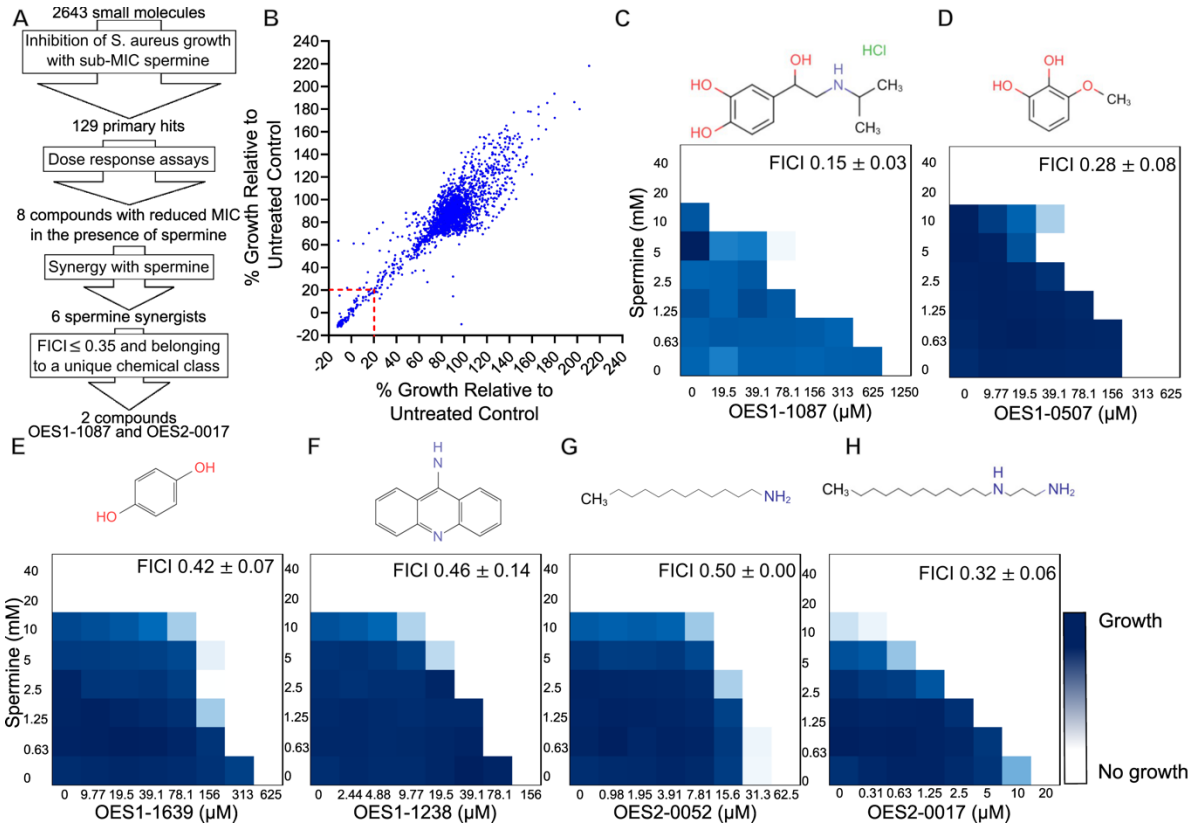

Figure 1. **High throughput screening identifies potent spermine synergists. A)** Workflow undertaken to identify chemical inhibitors of polyamine resistance. **B)** Replica plot of chemical screens performed to identify inhibitors of polyamine detoxification in *S. aureus* USA300. **C-H)** Chemical structures and representative checkerboard assays of the hits OES1-1087 (n=9) **(C)**, OES1-0507 (n= 4) **(D)**, OES1-1238 (n=3) **(E)**, OES1-1639 (n=3) **(F)**, OES2-0052 (n=3) **(G)**, and OES2-0017 (n=11) **(H)** with spermine against *S. aureus* USA300. FICI values are reported as mean ± standard deviation of the indicated number of replicates.

A chemogenomic screen to uncover the putative mechanism of spermine synergy. We undertook a genome-wide approach to identify the putative mechanism of spermine synergy by the screen hits, reasoning that a mutant with disruption in their putative target would exhibit both increased spermine susceptibility and loss or reduction in spermine-hit compound synergy. First, we sought to uncover the determinants of polyamine detoxification whose mutants would exhibit increased susceptibility to spermine by screening the Nebraska Transposon Mutant Library (NTML), a sequence-defined transposon mutant library covering the non-essential genome of *S. aureus* USA300 [42], against spermine at 1/8th and 1/16th the wild-type MIC. *speG*::Tn was sensitized to spermine, in agreement with previous reports [19], thus serving as an internal control for the screen. Mutants in another four determinants not previously linked to the response to

195 polyamines, *tcaA*::Tn, *cls*::Tn, *prmC*::Tn, and *pyrP*::Tn, were also sensitized to spermine
196 (Figure 2 A). Dose-response assays showed an 8-fold reduction in spermine MIC in
197 *speG*::Tn, and a decrease of the other four mutants at ½ MIC relative to the wild-type strain
198 (Supplementary Fig. 3). We constructed an in-frame unmarked deletion of *speG* given that
199 its transposon mutant had the most pronounced spermine MIC shift; Δ*speG* confirmed the
200 observed spermine susceptibility shift (Supplementary Fig. 3). *tcaA* encodes a predicted
201 transmembrane protein and is implicated in teicoplainin resistance [43]. *cls* encodes a
202 cardiolipin synthase involved in modulating the phospholipid composition of the membrane
203 [44]. *prmC* encodes a release factor methyltransferase, and *pyrP* an uracil-xanthine
204 permease. The molecular basis linking these determinants to polyamine response warrants
205 further investigation, which falls beyond the scope of this study. Notably, *sbnB*::Tn,
206 disrupted in a gene encoding an enzyme involved in the siderophore staphyloferrin B
207 biosynthesis [45], was initially identified in the screen and showed an 8-fold spermine MIC
208 reduction; however, Δ*sbnB* mutant was not sensitized to spermine (Supplementary Fig. 3).
209 Whole-genome sequencing and subsequent PCR analysis of the *sbnB*::Tn mutant revealed
210 an additional truncation of 46.8 kb comprising the SCC*mec* cassette and the ACME locus,
211 including *speG* and *mecA* (Supplementary Fig. 3); hence, *sbnB* was excluded from the
212 putative determinants list.
213 Next, we resupplied the hit compounds and conducted mini-checkerboard assays
214 with spermine against the five identified polyamine resistance determinants to detect loss or
215 reduction in synergy. The spermine synergistic interaction with OES2-0017 and OES1-1087
216 was lost or reduced in the Δ*speG* mutant (Figure 2 B), suggesting that SpeG is the putative
217 target of these compounds. Notably, spermine synergy was also lost in the other four de-
218 prioritized hit compounds against *ΔspeG* mutant (Supplementary Fig. 4), suggesting that all
219 six hits uncovered from the screens share a similar molecular target for spermine synergy.
220 We performed checkerboard assays with spermine and OES2-0017 or OES1-1087
221 against other *speG*$^+$ and *speG*$^-$ *S. aureus* strains. The tested strains included another
222 USA300 strain CMRSA-10 that encodes *speG* as well as two strains that do not encode
223 *speG* including the MRSA strain COL and the methicillin-sensitive *Staphylococcus aureus*
224 (MSSA) strain NCTC8325. The *speG*$^-$ strains, whether MRSA or MSSA, displayed a loss or
225 reduction in synergy between spermine and OES2-0017 or OES1-1087, phenocopying the
226 USA300 *ΔspeG* mutant (Figure 2 C-H). For both OES2-0017 and OES1-1087, CMRSA-10

227 displayed a similar synergistic phenotype to that observed in the other wild-type USA300
228 strain, JE2 (Figure 2 I and J). These results further suggest that OES2-0017 and OES1-
229 1087 are inhibiting SpeG activity, and that strains must encode *speG* to observe the
230 spermine synergistic phenotype.

231 Since SpeG is a spermine/spermidine acetyltransferase, we also tested spermidine
232 with either OES2-0017 or OES1-1087 in checkerboard assays. As expected, OES2-0017
233 and spermidine synergized with an FICI of 0.33 $\pm$ 0.06, such synergy was decreased in the
234 *ΔspeG* mutant (FICI = 0.48 $\pm$ 0.05) and *speG*$^-$ strains but not completely lost (Figure 2 K
235 and L and Supplementary Fig. 5). The same is observed with spermidine and OES1-1087
236 where the Δ*speG* mutant (FICI = 0.38 $\pm$ 0.09) or *speG*$^-$ strains showed reduced synergy
237 compared to wild-type USA300 (FICI = 0.17 $\pm$ 0.03) (Figure 2 M and N and Supplementary
238 Fig. 5). The results suggest that synergy between these compounds and spermidine is
239 mediated, at least in part, by SpeG inhibition.
240

241 **SpeG as the target of OES1-1087 and OES2-0017**. We sought to confirm the
242 SpeG inhibitory activity of the hit compounds in *in vitro* assays using purified His-tagged
243 recombinant SpeG. We used a colorimetric SSAT assay based on the quantification of
244 CoA-SH formed during the transfer of the acetyl group from acetyl-CoA, which is
245 proportional to the amount of the acetylated substrate (AcCoA) [46]. Under these
246 experimental conditions, we observed acetyltransferase activity for the native and not the
247 heat-inactivated SpeG when both spermine and spermidine were used as the test
248 substrates. Based on our results and previous analysis[47], SpeG displays Michaelis-Menten
249 kinetics with spermine as a substrate, allosteric kinetics with spermidine, and no activity with
250 putrescine, thus we estimated catalytic efficiency of each as K_m and $S_{0.5}$, respectively. The
251 SpeG K_m with spermine was 1312 $\pm$ 348.1 μM and $S_{0.5}$ with spermidine was 8669 $\pm$ 3031
252 μM (Supplementary Fig. 6). Catalytic efficiency of SpeG with spermine and spermidine as
253 substrates were 5.58E+03 and 2.51E+02 $M^{-1}s^{-1}$, respectively (Supplementary Fig. 6). These
254 results agree with previous reports showing that spermine is the preferred substrate of
255 SpeG, followed by spermidine and that SpeG does not acetylate putrescine [20,47].

256 Next, we confirmed that OES2-0017 and OES1-1087 inhibited acetyltransferase
257 activity of SpeG *in vitro* by performing enzymatic inhibition assays testing a dilution series of
258 each of the hits in the presence of either a single concentration or multiple concentrations of

259 substrate in a checkerboard-style format estimating IC_{50} and K_i, respectively. The IC_{50} of
260 OES2-0017 against SpeG was 34.82 $\pm$ 6.810 μM at ~ 1 x K_m of spermine and the K_i was
261 20.20 $\pm$ 3.446 μM when varying spermine concentrations both at a fixed saturating AcCoA
262 concentration (Figure 2 O and Supplementary Fig 7). The IC_{50} of OES1-1087 was 5508 $\pm$
263 1890 μM (at ~1 x K_m of AcCoA and a spermine ~ 1 x K_m concentration; Figure 2 P). OES1-
264 1087 did not exhibit inhibitory activity under a fixed AcCoA concentration and variable
265 spermine concentrations; however, at a fixed spermine concentration and variable AcCoA,
266 OES1-1087 inhibited SpeG with an estimated K_i of 5153 $\pm$ 2126 μM (Supplementary Fig.
267 8). K_i calculations were based on fitting the checkerboard-style data to the competitive
268 inhibition model for both inhibitors, which was further supported by Lineweaver-Burk
269 transformations (Supplementary Fig. 7 and 8). These values are slightly higher than
270 expected when compared to the concentrations exhibiting spermine synergy interactions in
271 whole-cell assays. However, this could be attributed to the *in vitro* cell-free experimental
272 conditions (i.e., buffer concentration, pH, temperature, etc.) that do not perfectly match the
273 conditions *in vivo,* which may be more optimal for catalysis. Of note, we use a high buffer
274 concentration (100 mM Tris-HCl) to prevent polyamine high pH-mediated cleavage of
275 Ellman's reagent, which is sensitive to high pH [48]. These data confirm that both OES2-0017
276 and OES1-1087 inhibit SpeG with OES2-0017 being more potent as a SpeG inhibitor,
277 matching with the whole-cell assay results (Figure 2 O and P and Supplementary Fig. 7 and
278 8).
279 *S. aureus* SpeG forms a dodecameric structure composed of two hexamers stacked
280 together in a ring-like structure [47]. Crystallographic data of SpeG from *S. aureus*, *Vibrio*
281 *cholerae*, and *E. coli* show spermine and spermidine bound in a pocket that expands two
282 adjacent monomers of the hexamer with a total of twelve binding sites in the dodecamer
283 [47,49,50]. When spermine, spermidine, or AcCoA bind to SpeG a conformational change
284 occurs, suggested to bring the AcCoA and polyamine molecule closer together for the
285 acetyl transfer [47,49,51,52]. Alignment of the crystal structures of *S. aureus* SpeG with and
286 without bound spermine depicts this conformational change and the spermine binding site
287 (PBD ID: 8FV0 and 5IX3, respectively; Figure 2 Q). We docked both OES2-0017 and
288 OES1-1087 in an unbiased manner to *S. aureus* SpeG (PBD ID: 5IX3). OES2-0017 is
289 predicted to bind between adjacent monomers at the same site as spermine and spermidine
290 with a ΔG of -6.636 Kcal/mol (Figure 2 R). This analysis aligns with our experimental data,

291 suggesting OES2-0017 is a competitive inhibitor of SpeG, competing with spermine to bind
292 the free enzyme.
293 *S. aureus* SpeG has not been crystalized in complex with CoA or AcCoA, but *V.*
294 *cholerae* SpeG has been co-crystallized with CoA, where it binds to the substrate binding
295 site between a cleft created by β4 and β5 strands and α-helices 3 and 4 [49]. Molecular
296 docking of *S. aureus* SpeG with AcCoA predicts it binds to the same site as in *V. cholerae*
297 (ΔG of -9.228 Kcal/mol; Figure 2 S). OES1-1087 was also predicted to bind this same
298 location (ΔG = -6.691 Kcal/mol; Figure 2 T). This prediction combined with our experimental
299 inhibition data led us to hypothesize that OES1-1087 is binding the same site as AcCoA and
300 is thus suggested to be acting as a competitive inhibitor. The lower affinity of OES1-1087 to
301 bind to the same site as AcCoA also suggests why OES1-1087 shows very weak inhibition
302 of SpeG. The *in vitro* enzymatic assays and protein docking data together suggest that
303 OES2-0017 and is OES1-1087 are competing with spermine or AcCoA, respectively to bind
304 SpeG, acting in a competitive manner.
305

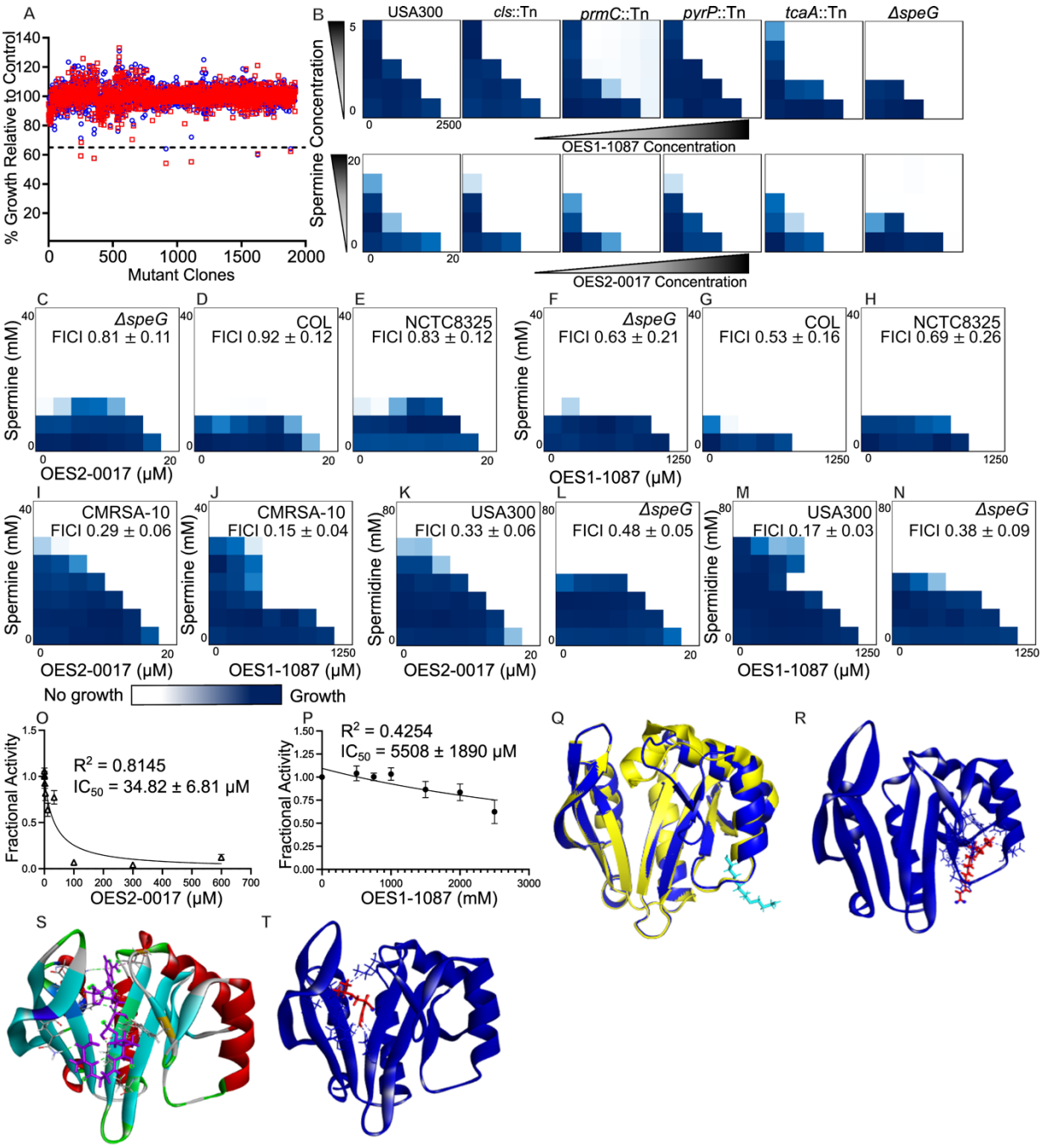

Figure 2. **OES2-0017 and OES1-1087 inhibit SpeG. A)** Chemogenomic screen of the Nebraska Transposon Mutant Library with spermine at 1/8th (red squares) and 1/16th (blue circles) the MIC. **B)** Mini-checkerboard assays performed by testing 2-fold dilutions of each of spermine and OES1-1087 or OES2-0017 against polyamine resistance determinants uncovered in **(A)** including *S. aureus* USA300, *cls*::Tn, *prmC*::Tn, *pyrP*::Tn, *tcaA*::Tn, and Δ*speG*. **C-N)** Representative checkerboard assays performed by testing 2-fold dilutions of each test compound. **C-E)** spermine and OES2-0017 against *S. aureus* Δ*speG* (n=9) **(C)**, COL (n=3) **(D)**, NCTC8325 (n=3) **(E)**. **F-H)** Spermine and OES1-1087 against *S. aureus* Δ*speG* (n=9) **(F)**, COL (n=4) **(G)**, NCTC8325 (n=4) **(H)**. **I)** OES2-0017 and spermine against CMRSA-10 (n=3), **J)** OES1-

1087 and spermine against CMRSA-10 (n=3). OES2-0017 and spermidine against **K)** USA300 (n=7) and **L)** Δ*speG* (n=6). OES1-1087 and spermidine against **M)** USA300 (n=3) and **N)** Δ*speG* (n=3). Checkerboards against Δ*speG* were performed on the same day as their counterparts against the wild-type strain shown in Figure 1. **O-P)** Colorimetric enzymatic assays conducted with 1 mM Acetyl Coenzyme A **(O)** or 0.75 mM Acetyl Coenzyme A **(P)** and 1500 μM spermine in the reaction mixture to evaluate the inhibition of OES2-0017 (n=7; **O)** and OES1-1087 (n=3**; P).** Data is represented as mean ± SEM for three independent experiments. **Q)** Alignment of *S. aureus* SpeG crystallized with (yellow; PDB ID: 8FV0) and without spermine (blue; PDB ID 5IX3). Molecular docking of **R)** OES2-0017, **S)** Acetyl-CoA, and **T)** OES1-1087 to *S. aureus* SpeG (PDB ID: 5IX3).

Uncovering parallel polyamine acetyltransferase mechanisms in USA300. Checkerboard assays with OES2-0017 and OES1-1087 revealed only a partial loss of synergy in the Δ*speG* mutant with the polyamine spermidine (Figure 2 K-N and Supplementary Fig. 5), suggesting other potential mechanisms may also be at play in the spermidine synergy and that these may also be targeted by the inhibitors. SpeG preferentially acetylates spermine while it acetylates spermidine with a lower affinity (Supplementary Fig. 5 and [20,47]). The lower affinity may contribute to a decreased ability to detoxify spermidine, possibly requiring other detoxification mechanisms that function in parallel to SpeG. Some bacteria encode SSATs distinct from SpeG, such as *B. subtilis* encoding two enzymes *paiA* and *bltD* [53,54] and *Enterococcus faecalis* encoding *pmvE* a homolog of *B. subtilis paiA* [25,53,54]. The presence of both *paiA* and *bltD* in *B. subtilis* provides evidence for the existence of parallel polyamine detoxification pathways. Further, a recent report observed an accumulation of *N*-acetylputrescine in the MSSA strain ATCC 25923, which does not encode SpeG; however, they did not identify the enzyme responsible for its production [21]. This further suggests that *S. aureus* may encode alternative polyamine acetyltransferases and that they may have activity towards different polyamines. We identified potential additional polyamine acetyltransferases in *S. aureus* by performing protein blast of the *B. subtilis* 168 strain sequences of BltD (Accession NP_390537.1) and PaiA (Accession NP_391095.1) against *S. aureus* to identify potential homologs. Blastp results for BltD revealed two hypothetical proteins of *S. aureus* USA300 FPR3757; SAUSA300_0441 with 29.76 percent identity (query coverage 54%, E value of $2e^{-}09$) and SAUSA300_2083 with 27.41 percent identity (query coverage 86%, E value of $5e^{-}09$). PaiA blastp results identified a homolog of *S. aureus* USA300 FPR3757; SAUSA300_2316 (denoted $PaiA_{Sa}$ herein), with 40.35 percent identity (99% query coverage, E value of 3 e^{-}

349 39). These *S. aureus* proteins have not been previously characterized functionally; all three
350 are annotated as ribosomal-protein-alanine acetyltransferases whereas SAUSA300_2083
351 and SAUSA300_2316 ($PaiA_{Sa}$) are also annotated as spermine/spermidine
352 acetyltransferase blt and PaiA, respectively.
353 To confirm or rule out SSAT activity of SAUSA300_2083, SAUSA300_0441, and
354 $PaiA_{Sa}$, we overexpressed and purified these enzymes to assess their activity *in vitro*. We
355 observed acetyltransferase activity of $PaiA_{Sa}$ when spermine and spermidine are used as
356 substrates but no activity with putrescine under the test conditions (Figure 3
357 A-C). $PaiA_{Sa}$ substrate affinity appears higher for spermine than spermidine (K_M = 2144 $\pm$
358 443.3 μM and 3996 $\pm$ 670.8 μM, respectively). Further, the catalytic efficiency of $PaiA_{Sa}$
359 with spermine as a substrate is ~7-fold higher than with spermidine (K_{cat}/K_M = 2.41E+03 and
360 3.47E+02 $M^{-1}s^{-1}$, respectively; Supplementary Fig. 9). Thus, these results suggest that
361 $PaiA_{Sa}$ is better at acetylating spermine at lower substrate concentrations than spermidine.
362 Notably, SAUSA300_2083 and SAUSA300_0441 did not exhibit actetyltransferase activity
363 against the polyamines spermine, spermidine or putrescine under the tested conditions
364 (Supplementary Fig. 9). These data suggest that the $PaiA_{Sa}$ is likely to function as a
365 spermine/spermidine acetyltransferase. Next, we tested the ability of OES2-0017 to inhibit
366 $PaiA_{Sa}$ spermine acetylation; the low spermidine acetylation signal precluded testing OES2-
367 0017 $PaiA_{Sa}$ inhibition with spermidine as a substrate. OES2-0017 inhibited $PaiA_{Sa}$ activity
368 exhibiting an IC_{50} value of 52.17 $\pm$ 5.897 μM and estimated K_i of 43.83 $\pm$ 6.693 (Figure 3 D
369 Supplementary Fig. 10). Next, we performed whole-cell spermine – OES2-0017 mini-
370 checkerboard assays against a *paiA*::Tn mutant, compared to the wild-type USA300,
371 revealing no loss of synergy in the *paiA*$_{Sa}$ mutant (Figure 3 E and F). SpeG, hypothesized to
372 be the primary spermine/spermidine detoxification enzyme in *S. aureus*, may have
373 compensated for the absence of $PaiA_{Sa}$, masking any phenotypic changes in the *paiA*$_{Sa}$
374 mutant; a *speG paiA*$_{Sa}$ double mutant may be required to assess the contribution of $PaiA_{Sa}$
375 in whole cells. Together, our results indicate that polyamine acetylation in *S. aureus* may
376 occur through $PaiA_{Sa}$ in addition to SpeG, serving as complementary acetyltransferase
377 enzymes, and that the SSAT function of both enzymes is inhibited by OES2-0017.

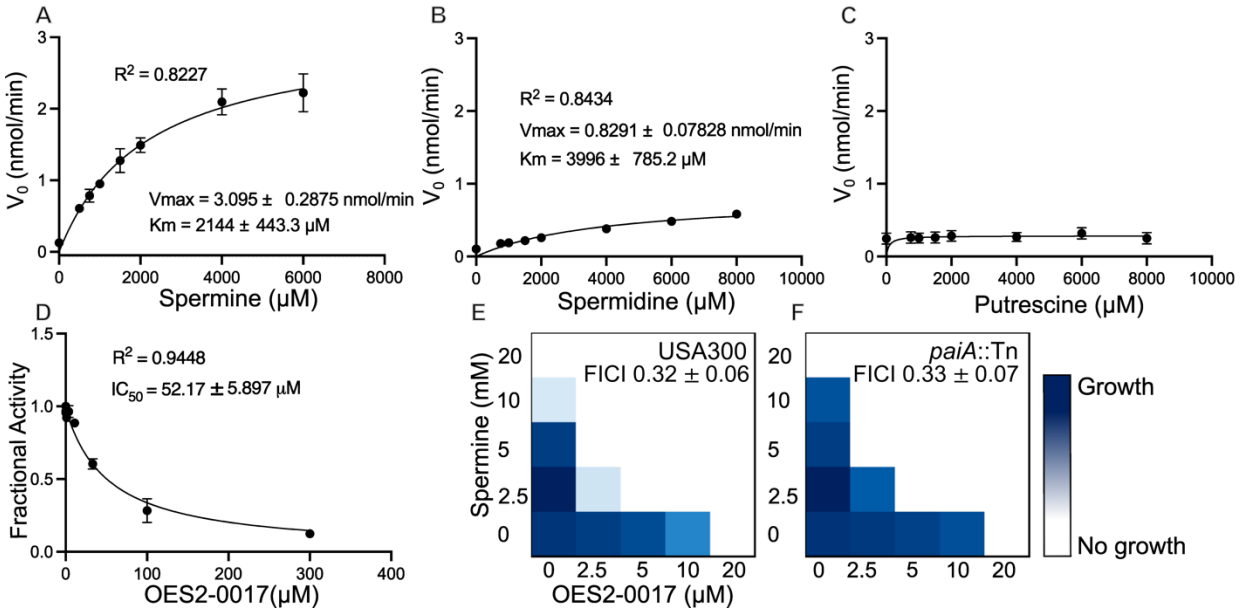

Figure 3. **Interaction of polyamines and OES2-0017 uncovers PaiA$_{Sa}$ as a spermine/spermidine acetyltransferase in *S. aureus*. A-C)** Steady-state enzymatic assays of PaiA$_{Sa}$ evaluate the acetylation activity in the presence of substrates **A)** spermine (n=6), **B)** spermidine (n=6), and **C)** putrescine (n=6). **D)** Enzymatic inhibition assay of PaiA$_{Sa}$ with spermine as a substrate by OES2-0017 (n=3). Results are represented as a mean ± SEM of three independent experiments. Representative checkerboard assays of spermine and OES2-0017 against *S. aureus* **E)** USA300 (n=11), **F)** *paiA*::Tn (n=3). FICI values are represented as mean ± standard deviation.

Uncovering the mechanism of growth inhibitory effects of OES2-0017. OES2-0017 and OES1-1087 exhibit growth-inhibitory effects at concentrations higher than those required to synergize with spermine; therefore, we hypothesized that this activity occurs via a second mode of action. Given its growth inhibitory activity at low micromolar range, we prioritized OES2-0017 to determine if growth inhibition was mediated through an essential protein target. We confirmed activity against *Bacillus subtilis,* a Gram-positive organism with high degree of genetic conservation with *S. aureus* (Supplementary Fig. 11). Then, we screened a knock-down library covering the essential genes of *B. subtilis* against three sub-inhibitory concentrations of OES2-0017, spanning ¼th-1/16th the wild-type MIC (Supplementary Fig. 11). While some mutants showed reduced growth in the presence of one or more of the tested sub-inhibitory concentrations, follow-up dose-response assays revealed that none of those mutants was more susceptible to OES2-0017 relative to the wild-type, suggesting the absence of an essential protein target.

Next, we hypothesized that the growth-inhibitory activity of OES2-0017 is due to an effect on membrane integrity in the absence of an essential protein target. Using a DiSC$_3$(5)

membrane integrity assay [55], we found that OES2-0017 permeabilized the membrane of USA300 at concentrations starting from its MIC (≥ 20 μM) in a concentration-dependent manner (Figure 4 A and B), suggesting membrane activity at high concentrations as the mechanism of growth inhibitory effects of OES2-0017. Notably, a $DiSC_3(5)$ assay with OES1-1087 did not have an observable effect on membrane integrity (Figure 4 C).

Next, we sought to check whether membrane disruption contributed to the observed synergy between OES2-0017 and spermine. We conducted a checkerboard-style $DiSC_3(5)$ assay with a combination of spermine and OES2-0017. OES2-0017 concentrations that correspond to the range of synergy (2.5-10 μM) resulted in no observable permeabilization (Figure 4 A and B). Like OES2-0017, spermine disrupted membrane integrity of USA300 at concentrations starting from its MIC against USA300 (Figure 4 B and Supplementary Fig. 12 A). We observed the similar membrane permeabilization with spermidine and putrescine (Supplementary Fig. 12 B and C) Large polyamine molecules were previously shown to permeabilize the outer membrane of Gram-negative bacteria [56]; however, we found no reports on similar effects on Gram-positive membrane integrity. Importantly, there was no significant effect on membrane integrity in the presence of the combination of OES2-0017 and spermine at concentrations where synergy is observed (Figure 4 B), suggesting that membrane permeabilization does not contribute to the observed synergy. Taken together, we revealed a dual mode of action of OES2-0017 with high concentrations leading to growth-inhibitory effects due to membrane perturbation and low concentrations synergizing with polyamines through inhibiting SpeG and other SSAT activity.

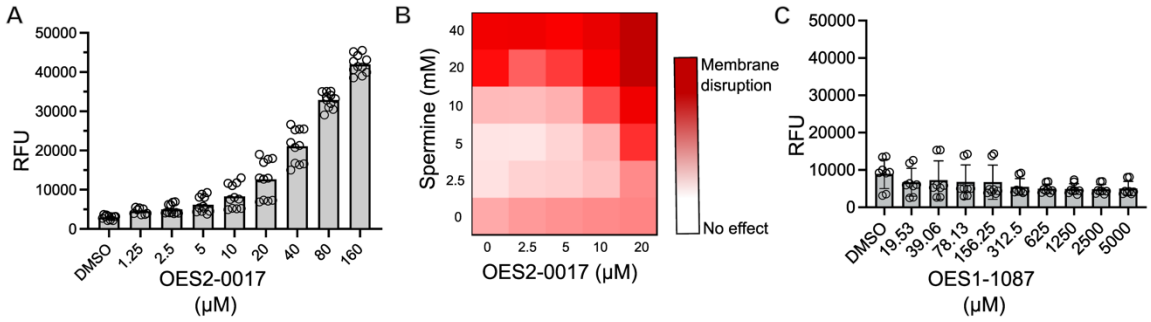

Figure 4. **Effects of OES2-0017 and OES1-1087 on *S. aureus* membrane integrity. A)** $DiSC_3(5)$ membrane permeabilization assay of OES2-0017 against *S. aureus* USA300. Results represented as mean relative fluorescence units (RFU) ± SEM for three independent experiments (n=11). **B)** A representative $DiSC_3(5)$ membrane permeabilization assay performed as a mini-checkerboard evaluating the combined effects of OES2-0017 and spermine. **C)** $DiSC_3(5)$ membrane permeabilization assay of OES1-1087 against *S. aureus* USA300. Results represented as mean ± SEM for three independent experiments (n=8).

431

432 **Broad-spectrum activity of OES2-0017 on clinically-relevant bacteria.** We conducted a
433 BLAST search of spermine/spermidine acetyltransferases using *S. aureus* SpeG as the
434 query, obtaining 94 amino acid sequences comprising eukaryotes, bacteria, and archaea.
435 Sequences were aligned using MUSCLE and a pairwise deletion of ambiguous positions
436 was performed for each sequence pair. The conservation of various SSATs was determined
437 by a maximum likelihood phylogenetic analysis (Supplementary Fig. 13). Although the main
438 purpose of such an analysis is to infer evolutionary history and relatedness, we used the
439 phylogenetic tree to visualize or infer sequence similarity between known
440 spermine/spermidine acetyltransferases. Our analysis reveals two main branches
441 originating from a common ancestor. The first branch shows archaea and (vertebrate)
442 eukaryotic organisms clustering together. This branch includes the human SAT1, rat, and
443 other mammalian SATs. The same branch also included *Acinetobacter baumannii* Dpa,
444 which was recently characterized as more closely resembling eukaryotic SSATs than
445 bacterial ones [57]. The second branch was divided into two sub-branches; the first contained
446 SpeG homologs in yeast while the second large sub-branch comprised bacterial SpeG. The
447 latter sub-branch included SpeG and other polyamine acetyltransferases that have
448 previously been characterized in both Gram-positive and Gram-negative organisms
449 including *Staphylococcus epidermidis* [23], *E. faecalis* (PmvE) [25], *Escherichia coli* [58], *V.*
450 *cholerae* [49], *Yersinia pestis* (PDB ID: 6D72), *B. subtilis* (BltD and PaiA) [53,54], and *Salmonella*
451 *enterica* serovar Typhimurium [24].

452 Given that SpeG has been implicated in virulence phenotypes in multiple bacteria
453 [14,24,59], we tested OES2-0017 being the most potent identified SpeG inhibitor against a
454 broad range of Gram-positive and Gram-negative bacteria and the pathogenic yeast
455 *Candida albicans* in checkerboard assays with spermine. The combination of OES2-0017
456 and spermine exhibited a synergistic interaction or an increase in spermine susceptibility in
457 *B. subtilis, E. faecalis, E. faecium, S. epidermidis, M. smegmatis, B. cenocepacia, E. coli, K.*
458 *pneumoniae, S.* Typhimurium, and *C. albicans* (Figure 5 A-K). In *A. baumannii* the
459 polyamine acetyltransferase Dpa preferentially acetylates 1,3-diaminopropane [57], which is a
460 diamine; therefore, we tested the diamine putrescine and OES2-0017 in combination.
461 OES2-0017 synergized with putrescine against *A. baumannii* (Figure 5 K). As in *S. aureus*,
462 OES2-0017 also inhibited the growth of all tested bacteria and *C. albicans* at the micromolar

range (Figure 5). Next, we tested the combination of spermine and OES2-0017 against the respective SSAT mutants of *E. coli* BW25113, *K. pneumoniae* MKP103, *S. enterica* sv. Typhimurium 14028s, and *B. subtilis* 168 (Figure 5. L-O). OES2-0017 no longer potentiated the effects of spermine in the SSAT mutants as opposed to their respective wild-type strains (Figure 5 L-O), suggesting OES2-0017 mediates its broad-spectrum spermine synergy through SSAT inhibition. Together, OES2-0017 exhibited broad-spectrum dual activity – polyamine synergy and growth inhibition – against Gram-positive and Gram-negative bacteria and fungi, including clinically relevant World Health Organization priority pathogens [60].

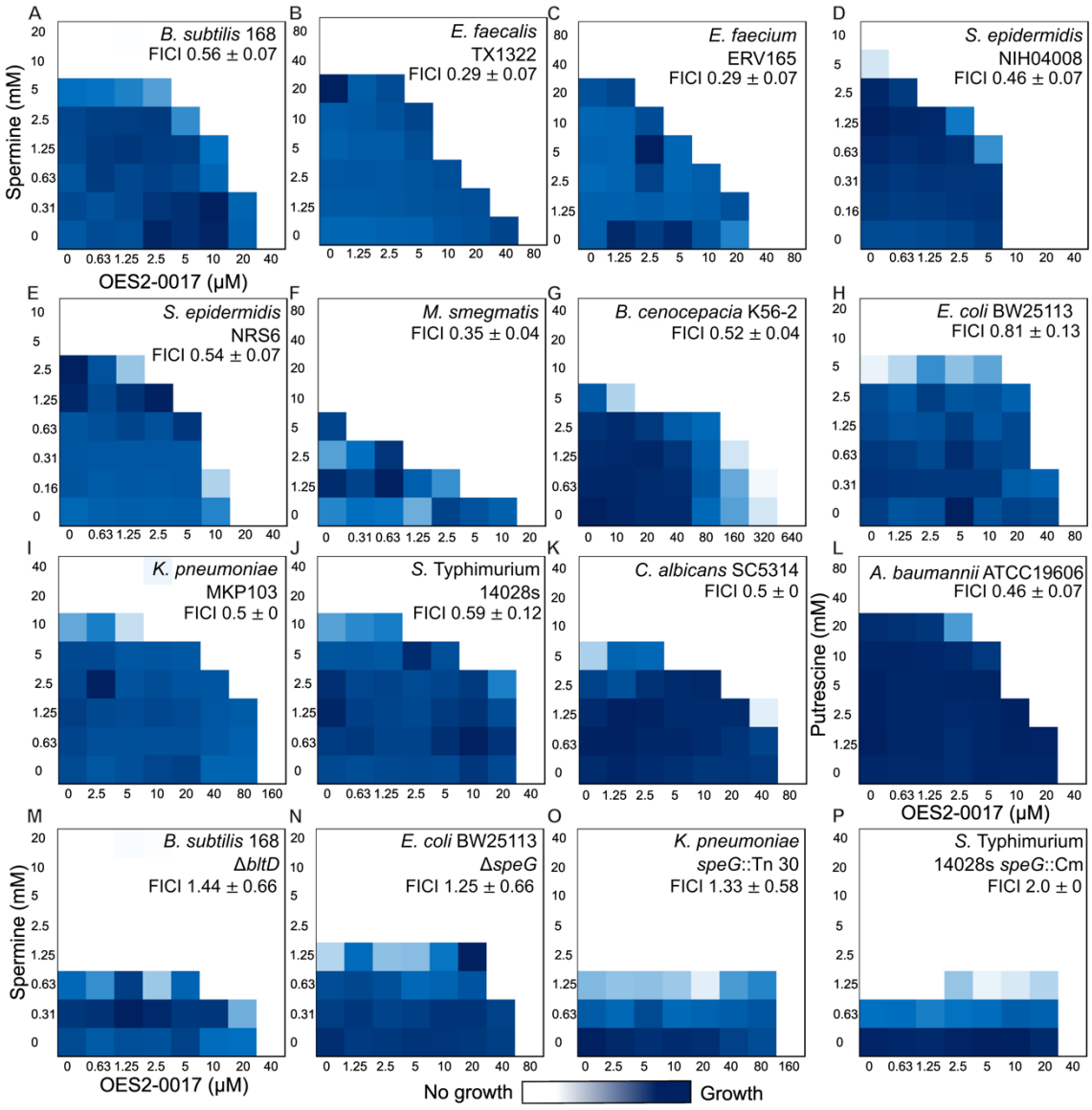

473 Figure 5. **OES2-0017 exhibits broad-spectrum activity.** Representative checkerboard assays of OES2-
474 0017 and spermine against **A)** *B. subtilis* 168 (n=4), **B)** *E. coli* BW25113 (n=4), **C)** *K. pneumoniae* MKP103
475 (n=4), **D)** *S.* Typhimurium 14028s (n=4), **E)** *E. faecalis* TX1322 (n=3), **F)** *E. faecium* ERV165 (n=3), **G)** *S.*
476 *epidermidis* NRS6 (n=3), **H)** *S. epidermidis* NIH04008 (n=3), **I)** *B. cenocepacia* K56-2 (n=3), **J)** *M.*
477 *smegmatis* (n=3), and **K)** *C. albicans* SC5314 (n=3). **L)** Putrescine and OES2-0017 checkerboard against
478 *A. baumannii* ATCC19606 (n=3). Representative checkerboard assays of spermine and OES2-0017
479 against spermine/spermidine acetyltransferase mutants **M)** *B. subtilis* Δ*bltD* (n=4), **N)** *E. coli* Δ*speG* (n=3),
480 **O)** *K. pneumoniae speG*::Tn30 (n=3), **P)** *S.* Typhimurium *speG*::Cm (n=3)**.** FICI values are represented as
481 mean ± standard deviation for the indicated number of replicates.

482
483

484 **Polyamine-mediated altered antibiotic susceptibility and the potential of OE2-0017 as**
485 **an antibiotic adjuvant.** Checkerboard assays of polyamines and representative antibiotics
486 from seven classes with diverse cellular targets revealed various polyamine-mediated
487 altered antibiotic responses (Supplementary Fig. 14). The three tested polyamines
488 synergized with the macrolide azithromycin while spermine synergized with the β-lactam
489 cefuroxime (Supplementary Fig. 14). The spermine β-lactam synergy matches previous
490 reports of the phenotype in *S. aureus* [26,28]. Similarly, polyamine synergy with macrolides has
491 been reported in the Gram-negative pathogens *K. pneumoniae* [30] and *E. coli* [28]. In *K.*
492 *pneumoniae* the synergistic interaction between azithromycin and putrescine is mediated
493 through the combined effects of putrescine-induced membrane perturbation and protein
494 synthesis inhibition via interaction at the ribosome [30]. The effects of polyamines on
495 ribosome function is well documented [61] and polyamines are known to interact with
496 biological macromolecules, including DNA, RNA, proteins, and phospholipids [16,62]. In
497 contrast, the three polyamines antagonized rifampicin and kanamycin whereas spermine
498 antagonized with vancomycin, defined as a FICI value ≥ 4 (Supplementary Fig. 14). The
499 mechanisms of the observed polyamine-mediated alterations to antibiotic susceptibility
500 warrant further investigation. On the other hand, we observed no alterations in daptomycin
501 or ciprofloxacin susceptibility in combination with the tested polyamines (Supplementary
502 Fig. 14).

503 Interestingly, the MIC of vancomycin is increased 4-fold when combined with
504 spermine (FICI = 4.69 ± 1.57), but the interaction is lost in a Δ*speG* mutant (FICI = 2.17 ±
505 0.26), suggesting that *S. aureus* requires a functional SpeG to use exogenous polyamines
506 to resist vancomycin (Figure 6 A and B). Supplementing a sub-inhibitory concentration of
507 OES2-0017 (2.5 μM) to a vancomycin-spermine checkerboard against *S. aureus* USA300
508 phenocopied the loss of antagonism observed against the Δ*speG* mutant (FICI = 1.59 ±

509 0.62; Figure 6 C). This phenotype is not due to a synergistic interaction between OES2-
510 0017 and vancomycin (Supplementary Fig. 15). Vancomycin is one of the first-line
511 antibiotics for the treatment of severe MRSA infections [63], suggesting the antagonism
512 between polyamines and vancomycin may be detrimental to MRSA treatment. Similarly, the
513 polyamine antagonistic interactions with rifampicin and kanamycin in USA300 were lost in
514 the Δ*speG* mutant and with supplementation of a sub-inhibitory concentration of OES2-0017
515 to the USA300 checkerboard (Figure 6 D-I). The loss of antagonism was not due to synergy
516 between OES2-0017 and kanamycin or rifampicin (Supplementary Fig. 15). While
517 kanamycin and rifampicin are not considered first-line monotherapies for MRSA infections,
518 they are often used in conjunction with vancomycin [64,65]; polyamines may reduce bacterial
519 susceptibility to these antibiotics. We also identified a synergistic interaction between
520 OES2-0017 and cefuroxime, where OES2-0017 lowered the MIC of the antibiotic to <16
521 μg/mL from 1024 μg/mL (FICI = 0.35 ± 0.13; Figure 6 J). OES2-0017 and azithromycin also
522 exhibited a slight potentiation effect against USA300 (FICI = 0.72 ± 0.21; Figure 6 K). A
523 similar potentiation effect was observed, where azithromycin synergized with OES2-0017
524 against *K. pneumoniae* [30]. These results suggest that OES2-0017 may serve as an
525 antibiotic adjuvant by preventing *S. aureus* from utilizing exogenous polyamines to resist
526 antibiotics (e.g., glycopeptides, aminoglycosides, and rifamycins) or by potentiating the
527 effects of antibiotics phenocopying the polyamine-mediated sensitization to certain
528 antibiotics (e.g., macrolides and β-lactams).

529 **OES2-0017 abrogates intracellular survival and may serve as an antivirulence agent.**

530 We tested the ability of OES2-0017 to clear *S.* Typhimurium infection of murine
531 macrophages since SpeG was previously shown to be necessary for the intracellular
532 replication of *S.* Typhimurium, where a *speG* knockout was attenuated in macrophages [24].
533 Bacterial load was significantly reduced in a gentamicin protection assay at both 4- and 15-
534 hours post-infection in the *speG::*Cm infected macrophages compared to the wild-type (p =
535 0.0286 and 0.0286, respectively; Figure 6 L and M). OES2-0017 treatment, whether pre- or
536 post-infection, reduced *S.* Typhimurium bacterial load in macrophages, similar to the levels
537 of recovered bacteria in the *speG*::Cm condition (Figure 6 L and M). Thus, OES2-0017
538 eradicated intracellular macrophage infection of the wild-type *S.* Typhimurium reducing its
539 virulence.

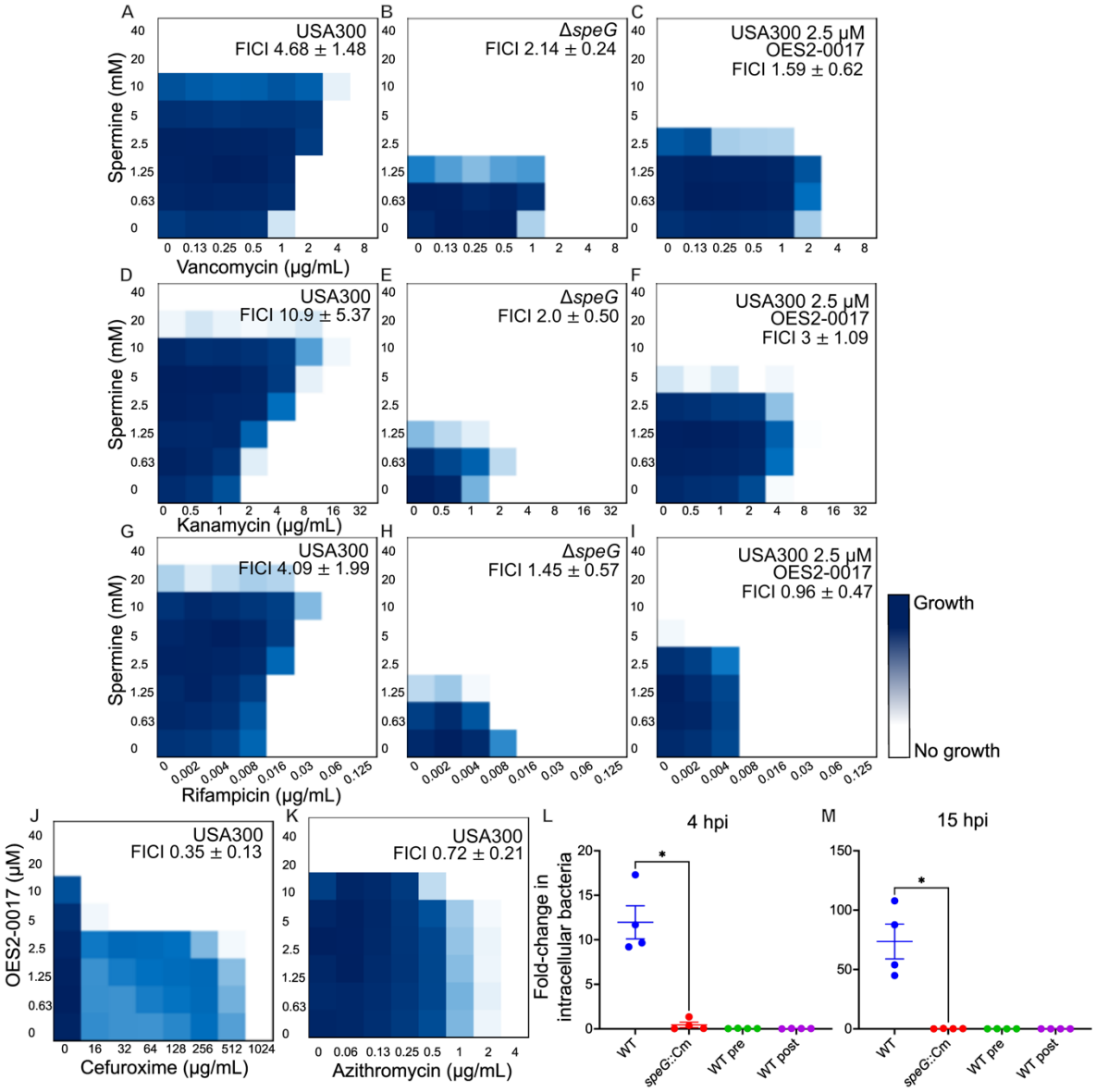

Figure 6. **The potential of OES2-0017 as an antibiotic adjuvant and an antivirulence agent.** Representative checkerboard assays of spermine and vancomycin **(A-C)**, kanamycin **(D-F)**, and rifampicin **(G-I)** against *S. aureus* **A, D, G)** USA300, **B, E, H)** Δ*speG*, and **C, F, I)** USA300 supplemented with a sub-inhibitory concentration of OES2-0017 where OES2-0017 abolishes the protective effect of polyamines from the antibiotics. Representative checkerboard assay of OES2-0017 and cefuroxime **(J)** and azithromycin **(K)** against *S. aureus* USA300, where OES2-0017 potentiates the antibiotic activity. **L** and **M)** murine macrophages treated with OES2-0017 before or after infection with *S.* Typhimurium 14028s or *speG*::Cm and bacterial colony forming units counted at **L)** 4 hours post-infection and **M)** 15 hours post-

551 infection. Data represent 3 independent experiments and statistical analysis was performed by Mann-
552 Whitney test (* signifies $p < 0.05$).

553 **Evaluation of OES2-0017 and OES1-1087 potential eukaryotic activity.** Given the
554 membrane activity of OES2-0017 against *S. aureus* (Figure 4 A and B), we sought to
555 evaluate its potential effects on mammalian cell membranes. To that end, we assessed the
556 hemolytic activity of OES2-0017 against sheep red blood cells. OES2-0017 exhibited
557 hemolytic effects, which are first observed at 160 μM with an increase at 640 μM reaching
558 an absorbance of roughly ½ that of the positive control (Triton X100) (Supplementary Fig.
559 16). The hemolytic effects do occur at a concentration significantly higher than what is
560 necessary to inhibit bacterial growth (8-fold higher than the MIC) or to synergize with
561 spermine through SpeG inhibition (512-fold higher than the lowest point of synergy with
562 spermine). Notably, OES1-1087 did not exhibit hemolytic effects at the concentrations
563 tested (Supplementary Fig. 16). To further evaluate the relative toxicity of OES2-0017 and
564 OES1-0187 toward eukaryotic cells, we also exposed MDCK epithelial cells to the
565 compounds and evaluated their ability to remain adhered to the tissue culture substratum
566 and viable. This analysis revealed that at the *S. aureus* USA300 MIC (1250 μM) OES1-
567 1087 treated cells remain adhered and are refractory to viability dye staining. In contrast,
568 OES2-0017 treated cells detach from the tissue culture substratum at the MIC (20 μM);
569 however, this effect is significantly diminished at ½ the MIC. Moreover, under these same
570 conditions, OES2-0017 treatment does not result in loss of cell viability (Supplementary Fig.
571 17). Altogether, these data indicate that at the concentrations employed in our study
572 significant toxicity towards host cells would not occur.

573 Next, we assessed the activity of OES2-0017 and OES1-1087 against the human
574 spermine/spermidine acetyltransferase, SAT1. SAT1 is a dimer in solution with one
575 monomer seemingly self-acetylating a lysine residue and the other binding polyamines for
576 acetylation [66]. SpeG and SAT1 are located on two separate branches of the phylogenetic
577 analysis (Supplementary Fig. 13), suggesting a distant relation. A protein alignment by
578 PyMOL 3.0 revealed monomers of the SpeG and SAT1 apoenzymes align well with minor
579 differences in their tertiary structures (PDB ID 5IX3 and 2B5G, respectively; Figure 7 A).
580 However, differences between aligned SpeG and SAT1 are greater when both are bound to
581 substrate (PDB ID 8FV0 and 2BD4, respectively; Figure 7 B). First, we overexpressed and
582 purified SAT1 enzyme and confirmed its acetyltransferase activity *in vitro* with spermine.

583 SAT1 demonstrated higher substrate specificity (K_M = 73.10 ± 8.328 μM) and high catalytic
584 efficiency (K_{cat}/K_M = 1.28E+05 $M^{-1}s^{-1}$) towards spermine than SpeG (K_M = 1312 ± 348.1 μM
585 and K_{cat}/K_M = 5.58E+03 $M^{-1}s^{-1}$; Supplementary Fig. 18). Our results are in agreement with
586 previous kinetic characterization and the relative activities of both enzymes [20,67]. We then
587 tested the ability of OES2-0017 and OES1-1087 to inhibit SAT1. The IC_{50} of OES2-0017
588 against SAT1 was 26.39 ± 6.411 μM (Figure 7 C), whereas OES1-1087 did not inhibit SAT1
589 under any of the tested conditions (Supplementary Fig. 18). Although, OES2-0017 can
590 inhibit SAT1 activity, this may not prove detrimental to human cells. Multiple studies have
591 employed the SSAT knockout mice and the non-specific SSAT inhibitor Berenil in *in vivo*
592 mouse models, observing no toxic effects to mice [68-70]. On the other hand, SAT1 inhibition
593 might have other potential therapeutic uses. Altered polyamine metabolism has been
594 implicated in many human diseases and conditions, including cancer, osteoporosis, and
595 ischemia/reperfusion leading to acute kidney injury [68,70-73] with SAT1 being previously
596 suggested as a promising drug target [66,74].

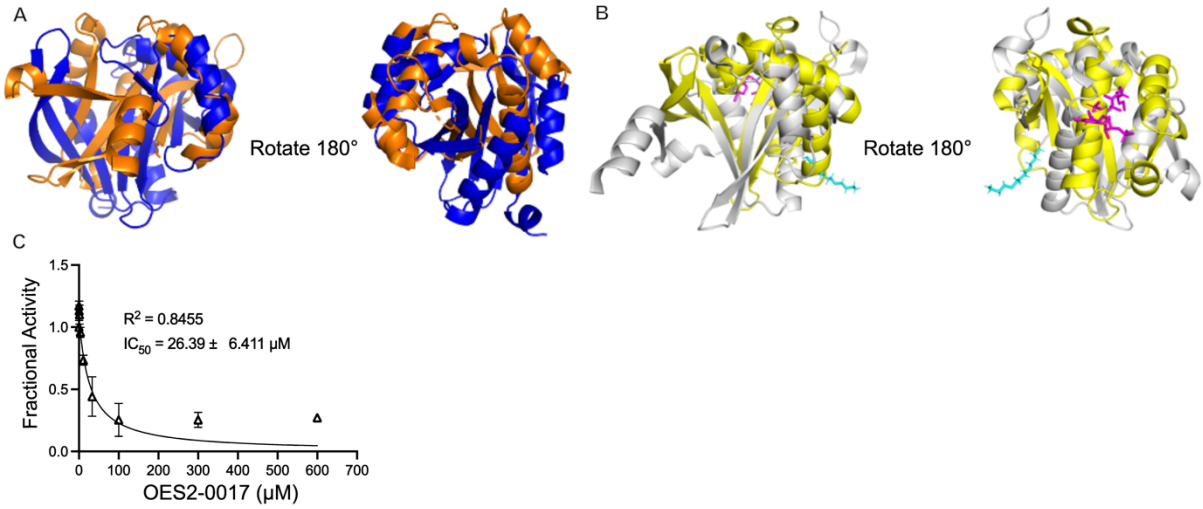

597

598 Figure 7. **Effects of OES2-0017 on human SSAT. A)** Structural alignment of human SAT1 (PDB
599 ID 2B5G) represented with orange, and *S. aureus* SpeG (PDB ID 5IX3) represented with blue
600 apoenzymes. **B)** alignment of human SAT1 (PDB ID: 2B4D; grey) co-crystallized with Coenzyme A
601 (magenta) and spermine and *S. aureus* SpeG (PDB ID: 8FV0; yellow) co-crystallized with spermine
602 (cyan). Structural alignments were performed using PyMOL 3.0. **C)** Enzymatic inhibition assay performed
603 against human SAT1 with excess AcCoA (0.25 mM) and 75 μM spermine (≈ K_M).

604 **Small-scale structure activity relationship of OES2-0017 suggests the**
605 **structural components necessary for activity.** We performed a small-scale structure

606 activity relationship (SAR) study of OES2-0017 by testing analogs thereof to identify the
607 active moiety of OES2-0017 and detect preferential inhibitory activity against either SpeG or
608 SAT1. The analyses included compounds with varied length of the saturated alkyl chain R_1
609 and one of three R_2 (a proton, an aminoethyl group, or an aminopropyl group) attached on
610 either side of an amine group (Table 1). First, we tested each of the compounds in whole-
611 cell assays in combination with spermine to assess their growth inhibitory and polyamine
612 synergy effects against *S. aureus* USA300. We observed a general reduction in the MIC of
613 the compound as the length of R_1 and R_2 increased (Table 1). Spermine synergy appeared
614 to be dependent on both the length of the alkyl chain and the addition of either the
615 aminoethyl or aminopropyl group. The FICI value decreased (indicating a greater degree of
616 synergy) as the length of the alkyl chain increased; for example, OES2-0047 with R_1 as a
617 proton exhibited no synergy (FICI = 0.88 $\pm$ 0.13) whereas OES2-0052 with R_1 $(CH_2)_5CH_3$
618 showed synergy (FICI = 0.50 $\pm$ 0). The synergistic interaction is further improved when the
619 primary amine is changed to a secondary one with an aminoethyl or aminopropyl; this trend
620 is exemplified in OES2-0046 (R_2 = H; FICI = 0.58 $\pm$ 0.12), OES2-0085 (R_2 = aminoethyl;
621 FICI = 0.56 $\pm$ 0.05), and OES2-0045 (R_2 = aminopropyl; FICI= 0.38 $\pm$ 0).

622 The analogs that synergized with spermine lost the synergy against the Δ*speG*
623 mutant (Table 1), suggesting their synergy is mediated through SpeG inhibition similar to
624 OES2-0017. The analogs that did not exhibit synergy in whole-cell assays are hypothesized
625 to have no SpeG inhibitory activity. Therefore, we tested each compound in enzymatic
626 assays, against both SpeG and SAT1 and estimated K_i values using equation 1 (materials
627 and methods). OES2-0017 remains the most potent inhibitor of SpeG, K_i = 16.25 $\pm$ 3.27 μM
628 with OES2-0052 being the second most potent, K_i = 74.6 $\pm$ 18.28 μM (Table 1 and
629 Supplementary Fig. 19). OES2-0047 and OES2-0046 do not synergize in whole-cell assays
630 and do not inhibit SpeG *in vitro*; thus, they serve as controls to validate the correlation
631 between *in vitro* and whole-cell assays and that our lead compound is targeting and
632 inhibiting SpeG.

633 OES2-0017 inhibited SAT1 with a K_i of 13.03 $\pm$ 4.69 μM, similar to that of SpeG, but
634 the K_i of OES2-0052 is roughly 2-fold higher in SAT1 than SpeG (160.22 $\pm$ 50.45 μM and
635 74.6 $\pm$ 18.28 μM, respectively; Table 1). Similarly, OES2-0077 has almost a two-fold higher
636 K_i against SAT1 than SpeG (743.34 $\pm$ 250.46 and 397.89 $\pm$ 113.0 μM, respectively).

637 Further, two of the tested compounds only inhibited SpeG (OES2-0085 at K_i = 592.08 ±
638 126.15 μM and OES2-0086 at K_i = 559.42 ± 201.51 μM) and not SAT1, in contrast, SAT1
639 activity increased at the highest tested concentrations of these analogs (Supplementary Fig.
640 19). Notably, OES2-0045 which synergized with spermine in whole-cell assays (FICI = 0.38
641 ± 0 μM), suggesting SpeG inhibitory activity, showed no inhibition in the *in vitro* enzymatic
642 assays; however, it inhibited SAT1 (K_i = 227.99 ± 49.73μM; Table 1 and Supplementary
643 Figure 19). These results showing differential activity of some analogs against both
644 enzymes suggest a potential to improve specificity of an inhibitor towards SpeG. Docking
645 the analogs to SpeG or SAT1 revealed that each is expected to bind to the same site as
646 spermine/spermidine, suggesting that all analogs would act in a similar mechanism as
647 OES2-0017 (Supplementary Fig. 20).

648 Given that the compounds also exhibit growth-inhibitory effects, we simultaneously
649 evaluated their hemolytic activity. Hemolytic activity aligned with the MIC data where the
650 concentration required to lyse red blood cells was observed at lower concentrations for
651 compounds with a longer alkyl chain (R_1 = $(CH_2)_3CH_3$ or $(CH_2)_5CH_3$) and with an aminoethyl
652 or aminopropyl group at R_2 (Table 1 and Supplementary Fig. 21). Hemolysis for the SpeG
653 inhibitory compounds OES2-0085 and OES2-0077 occurred at 1280 μM (~2-fold higher
654 than their MICs), while hemolytic activity of OES2-0086, and OES2-0052 was observed at ~
655 4-fold higher than their MICs (640 and 320 μM, respectively; Table 1 and Supplementary
656 Fig. 21). We observed no hemolytic activity of two analogs with high MIC values OES2-
657 0047 and OES2-0046 (Table 1 and Supplementary Fig. 21). The same compounds were
658 also analyzed for their impact on MDCK monolayers which revealed, at their respective
659 MICs against *S. aureus* USA300 and 1 step below (½ MIC), the compounds did not overtly
660 intoxicate eukaryotic cells (Supplementary Fig. 22). Given the promising results of OES2-
661 0052 being more potent against SpeG than SAT1 and lacking observable toxicity against
662 eukaryotic cells, we tested if this compound retains the potential adjuvant activity of OES2-
663 0017. OES2-0052 abolishes the protective effect of spermine towards vancomycin,
664 kanamycin, and rifampicin, and potentiates the activity of cefuroxime (Supplementary Figure
665 23). This analysis provides a foundation for a larger scale targeted lead optimization to
666 improve the potency of SpeG inhibition, while reducing the hemolytic and SAT1 inhibitory
667 activity.

668 Table 1. **Small scale structure activity relationship study of OES2-0017.** SAR study compounds were
669 tested in combination with spermine against *S. aureus* USA300 and Δ*speG*. FICI values are calculated as
670 the mean ± standard deviation of at least three replicates, unless otherwise specified. Inhibitory activity
671 against both SpeG and SAT1 was evaluated in colorimetric enzymatic assays to determine K_i values
672 estimated by the Cheng-Prusoff equation and reported with relative error. Hemolytic activity of each
673 compound was tested against sheep red blood cells.

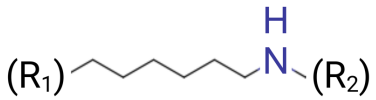

674

Inhibitor	R_1	R_2	MIC (μM)	FICI USA300	FICI Δ*speG*	SpeG K_I (μM)	SAT1 K_I (μM)	Observed hemolysis (μM)
OES2-0047	H	H	2500	0.88 ± 0.13 (n=2)	1.38 ± 0.63 (n=2)	N/A	N/A	None
OES2-0046	CH_2CH_3	H	5000	0.58 ± 0.12	0.92 ± 0.12	N/A	N/A	None
OES2-0085	CH_2CH_3	$(CH_2)_2NH_2$	625	0.56 ± 0.05	1.0 ± 0	592.08 ± 126.15	N/A	1280
OES2-0045	CH_2CH_3	$(CH_2)_3NH_2$	1250	0.38 ± 0	0.67 ± 0.12	N/A	227.99 ± 49.73	1280
OES2-0077	$(CH_2)_3CH_3$	H	625	0.50 ± 0	0.83 ± 0.12	397.89 ±113.0	743.34 ± 250.46	1280
OES2-0086	$(CH_2)_3CH_3$	$(CH_2)_2NH_2$	156.25	0.42 ± 0.12	0.83 ± 0.12	559.42 ± 201.51	N/A	640
OES2-0052	$(CH_2)_5CH_3$	H	62.5	0.50 ± 0	1.25 ± 0.54	74.60 ± 18.28	160.22 ± 50.45	320
OES2-0017	$(CH_2)_5CH_3$	$(CH_2)_3NH_2$	20	0.33 ± 0.06 (n=11)	0.75 ± 0 (n=9)	16.25 ± 3.27	13.03 ± 4.69	160

675

676 **Conclusions**

677 We undertook a chemical screen to identify inhibitors of polyamine detoxification,
678 and uncovered two lead compounds, OES2-0017 and OES1-1087, that show growth
679 inhibition and synergy with spermine. A chemogenomic screen and *in vitro* enzymatic
680 assays revealed that both compounds inhibit the spermine/spermidine acetyltransferase
681 SpeG. The most potent of the two, OES2-0017 with activity at the low micromolar
682 concentration range, inhibited bacterial growth via membrane perturbation. We also
683 observed the growth inhibitory and spermine synergistic effects of OES2-0017 in a broad-

684 spectrum of Gram-positive and Gram-negative bacteria, including *E. faecalis, E. faecium, B.*
685 *cenocepacia, K. pneumoniae,* and *A. baumannii*, and the pathogenic yeast *C. albicans*.
686 Synergy between spermidine and OES2-0017 was not completely lost in a USA300 Δ*speG*
687 mutant, suggesting other underlying polyamine detoxification targets, which prompted us to
688 search for SSATs homologous to *B. subtilis* PaiA and BltD. We found $PaiA_{sa}$, characterized
689 its SSAT activity *in vitro*, and showed that OES2-0017 inhibited its activity. OES2-0017
690 prevented intracellular survival of *S.* Typhimurium in murine macrophages, phenocopying a
691 *speG* deficient mutant. Further, OES2-0017 synergized with cefuroxime and potentiated
692 azithromycin activity against *S. aureus*. This potentiation effect with azithromycin is similar
693 to previous work in *K. pneumoniae* [30]. OES2-0017 also abolished the ability of *S. aureus* to
694 use exogenous polyamines to resist antibiotic treatment. Finally, we performed a small-
695 scale SAR study and identified compounds with differential activity towards the human
696 SAT1 and *S. aureus* SpeG, including OES2-0086 and OES2-0052. Together, the growth
697 inhibitory effects of the inhibitors identified herein suggest their potential use as stand-alone
698 antimicrobials and their SSAT inhibitory effects, shown to prevent *S.* Typhimurium survival
699 in macrophages, suggest they may serve as antivirulence agents. The synergy with some
700 antibiotics and ability to prevent exogenous polyamine-mediated resistance to other
701 antibiotics in *S. aureus* suggest OES2-0017 may also be used as an antibiotic adjuvant.
702 Polyamine analogs have previously been demonstrated to have antiparasitic,
703 anticancer [74-76], and antibacterial properties [77-79]; however, the previously tested analogs
704 differ in structure from OES2-0017 and the other polyamine analogs tested in this study.
705 Antibacterial polyamines described to date include mono- and bis-acyl polyamines, amine
706 steroidal derivatives [77], and diacylpolyamines with aromatic head groups [78]. One study
707 tested linear polyamine analogs, similar to OES2-0017, and revealed bactericidal and β-
708 lactam potentiating activity; however, the mechanism of growth inhibition and antibiotic
709 potentiation were not discussed [79]. Notably, several polyamine analogs were shown to
710 inhibit polyamine biosynthesis, transport, and catabolism [75,76]. As such, in addition to
711 screening a diverse small molecule library, we also undertook a targeted approach of
712 screening a library of polyamine analogs for activity against polyamine detoxification
713 enzymes. Indeed, this rationale-based approach showed a higher hit rate and higher
714 potencies compared to the unbiased approach although both screens identified SSAT
715 bioactives.

716 Specific bacterial SSAT inhibitors have not been identified previously. Notably,
717 berenil (diminazene aceturate) was shown to inhibit SSAT and has been used *in vivo* in
718 murine models for this purpose [70]. *In vitro* assays against human SSAT suggested berenil is
719 a potent competitive inhibitor of spermidine with a K_i of 2.0 μM [80]; however, berenil also
720 inhibits rat S-adenosyl-L-methionine decarboxylase and mouse polyamine oxidase [80,81].
721 Activity against multiple enzymes may explain the toxic effects observed during
722 intramuscular injection of camels with 10 mg/kg berenil [82]; however no toxic effects were
723 observed in mice dosed at 16 mg/kg weekly for six weeks [70] or with a single intraperitoneal
724 or intramuscular dose of 3.5, 10, or 20 mg/kg [82,83]. Aside from the SSAT activity, berenil was
725 shown to have other activities, including immunomodulatory[84] and cardioprotective[85]
726 activities, and is used in veterinary medicine mostly for parasitic infections albeit the exact
727 underlying mode of such activity is not fully elucidated but has been associated with the
728 connection of its aromatic diamidine to the kinetoplast DNA (kDNA) of the trypanosomes[86].
729 Our study provides insights that may lead to the development of specific bacterial SSAT
730 inhibitors. Although OES2-0017 caused the detachment of MDCK epithelial cells and
731 hemolytic activity at the MIC and 4X MIC against *S. aureus* USA300, respectively, SpeG-
732 inhibitory activity of the compound was observed as low as 1/32nd the MIC, suggesting a
733 concentration range within which OES2-0017 may remain efficacious while avoiding
734 potential adverse effects. Future studies will further assess the potential toxicity of OES2-
735 0017 and its analogs and their interaction with other polyamine-related enzymes using
736 natural polyamines as substrate.
737 We also identified OES1-1087 (isoproterenol) as a spermine synergist.
738 Isoproterenol is a β1- β2-adrenergic agonist used in the treatment of heart block, heart
739 failure, and cardiac arrest [87]. Its identification in our chemical screen serves as an example
740 of potential drug repurposing for the treatment of bacterial infections. Time and money
741 spent on drug development are drastically reduced by repurposing as pharmacodynamic,
742 pharmacokinetic, and toxicity profiles of the drugs are already known [88]. Our results indicate
743 that isoproterenol also inhibits SpeG, albeit with much lower potency than OES2-0017, and
744 exhibits growth inhibitory activity. Importantly, it did not show detectable activity against the
745 human SAT1 and no hemolytic activity or adverse effects on MDCK epithelial cell
746 adherence or viability.

747 The cellular concentrations of polyamines in mammalian cells vary across tissues
748 and physiological conditions; however, the total polyamine content is generally assessed to
749 be in the mM range [16]. Polyamines are known to bind to macromolecules, such as DNA,
750 RNA, phospholipids, and ATP, so levels of free intracellular polyamines are not definitive [16].
751 In polyamine-producing bacteria, the contents of intracellular polyamines have been
752 reported as high as 30 mM [16]. Importantly, polyamine concentrations in the host further
753 increase ~2-fold in response to infection [14]. As such, bacteria are likely to encounter
754 polyamines during infection or in their surrounding environment at concentrations similar or
755 higher than those tested in this study. Further, the detrimental effects of *speG* or alternative
756 SSAT mutations on bacterial virulence [14,24,25] suggest that the levels of polyamines within
757 the host are comparable to those used *in vitro* at which polyamine susceptibility and
758 synergy with the inhibitors were observed in this study. Therefore, given that OES2-0017
759 inhibits *speG,* it will likely reduce the ability of bacteria to withstand host polyamines
760 produced at the site of infection, suggesting it may allow these host compounds to help
761 clear infection serving as antivirulence agent.
762 *In vitro* enzymatic assays suggest that OES2-0017 is relatively equipotent against
763 both SpeG and SAT1 suggesting potential activity against the human enzyme *in vivo*. SAT1
764 inhibitors have other potential therapeutic uses including disrupting tumor growth, protection
765 from kidney injury following ischemia-reperfusion injury, and preventing osteoporosis
766 [66,68,70,74]. Notably, there were two analogs of OES2-0017, OES2-0085 and OES2-0086, that
767 showed inhibitory activity against SpeG but not SAT1 and another two, OES2-0077 and
768 OES2-0052, which were more potent inhibitors of SpeG than SAT1. Although these analogs
769 have lower inhibitory activity than OES2-0017, they and other analogs from our analysis can
770 guide future SAR studies to optimize the inhibition of SpeG while limiting activity against
771 SAT1.

772 *S. aureus* was not previously known to have an SSAT except for strains that
773 acquired SpeG, such as USA300. Notably, the USA300 Δ*speG* and other *S. aureus* strains
774 that do not harbor *speG* (e.g., COL and NCTC8325) are only 4-fold and 8-fold more
775 susceptible to spermidine and spermine, respectively, compared to wild-type USA300,
776 suggesting a potential for another detoxification mechanism. Here, we identified $PaiA_{Sa}$, a
777 homolog of *B. subtilis* spermine/spermidine acetyltransferase PaiA, in *S. aureus,* providing
778 its first experimental characterization as an additional SSAT in *S. aureus*. SpeG appears to

779 be more dominant with a greater shift in polyamine susceptibility observed in a Δ*speG*
780 mutant than *paiA*$_{Sa}$::Tn; the contribution of PaiA$_{Sa}$ to polyamine resistance in whole cells
781 requires assessment in a *speG paiA*$_{Sa}$ double mutant in USA300 or a single *paiA*$_{Sa}$ mutant
782 in a *speG*$^{-}$ *S. aureus* strain. We further showed that OES2-0017 can inhibit PaiA$_{Sa}$ *in vitro.*
783 This work provides insights into understudied aspects of chemically mediated host-
784 pathogen interactions. We discovered two novel inhibitors of spermine/spermidine *N*-
785 acetyltransferase. The discovered inhibitors have potential application as stand-alone
786 antimicrobials, antivirulence agents, or antibiotic adjuvants. This work provides antimicrobial
787 compounds with a novel mechanism for the fight against multidrug-resistant priority
788 pathogens.

789 **Materials and methods**

790 **Bacterial strains and reagents.** Table S1 and S2 list strains, plasmids and primers
791 used in this work. Bacteria were grown in cation-adjusted Mueller Hinton medium (MHB) at
792 37°C, except for *Enterococcus faecalis* and *Enterococcus faecium*, which were grown in
793 Tryptic Soy Broth and *Mycobacterium smegmatis,* which was grown in Luria Broth.

794 **Antimicrobial susceptibility testing.** Minimum inhibitory concentration (MIC) and
795 checkerboard assays were performed using the CLSI broth microdilution technique [8]. The
796 fractional inhibitory concentration indices (FICI) were calculated as FICI = ($MIC_{drug\ A}$ in
797 combination/$MIC_{drug\ A}$ alone) + ($MIC_{drug\ B}$ in combination)/$MIC_{Drug\ B}$ alone). FICI values were
798 interpreted as synergy when FICI ≤ 0.5, no interaction when 1 ≤ FICI ≤ 4, and antagonism
799 when FICI > 4.0.

800 **Chemical screen and polyamine analog library assembly.** We assembled a
801 library of polyamine analogs by selecting commercially available (Aldrich Market select)
802 analogs with at least 60% structural similarity to substrates and products of polyamine
803 biosynthesis and detoxification enzymes in bacteria. This library was screened at 20 μM in
804 the presence and absence of spermine at 1/4th the wild-type MIC. Library compounds were
805 added to 96-well plates and filled with inoculated MHB. We also screened a library of
806 previously approved drugs and natural product derivatives (Spectrum collection,
807 MicroSource Inc.) at 20 μM against the wild-type USA300 strain in the presence of
808 spermine at 1/4th the wild-type MIC. Compounds were administered to 384-well plates
809 containing inoculated MHB with spermine using the Biomatrix BM5-BC (S&P Robotics inc.).

810 Plates were incubated at 37°C, and bacterial growth was determined turbidimetrically after
811 24 hours.
812 ***S. aureus* Nebraska Transposon Mutant Library (NTML) screen.** Overnight
813 cultures of the NTML [42] were prepared in 384-well plates using Biomatrix BM5-BC (S&P
814 Robotics inc.) in MHB containing 5 µg/mL erythromycin. The following day, MHB containing
815 1/8th and 1/16th the wild-type USA300 MIC of spermine were inoculated using the Biomatrix
816 BM5-BC. Plates were grown at 37°C, and OD_{600} was read after 24 h.
817 ***B. subtilis* CRISPRi essential gene knockdown library screen.** Overnight
818 cultures of the library [89], were prepared in 96-well plates using Biomatrix BM5-BC (S&P
819 Robotics inc.) in MHB containing 6 µg/mL chloramphenicol. The following day, MHB
820 containing OES2-0017 at the wild-type MIC and at 2-fold dilutions to 1/16th the MIC and in
821 the absence of OES2-0017 were inoculated using the Biomatrix BM5-BC. The experiment
822 was performed with 0.05% xylose (allowing low level of *dcas9* expression) and without
823 xylose (allowing basal *dcas9* expression). Plates were incubated at 37°C, and OD_{600} was
824 read after 24 h.
825 **General molecular techniques.** Unmarked in-frame deletion of speG was
826 performed using the temperature-sensitive allelic exchange plasmid pJB38 [90].
827 Approximately 1-kb upstream and downstream of *speG* were PCR amplified and the
828 upstream fragment digested with EcoRI and BamHI (New England Biolabs), and the
829 downstream fragment digested with EcoRI and SalI (New England Biolabs). pJB38 was
830 digested with BamHI and SalI and fragments were ligated with T4 DNA ligase. The resultant
831 deletion plasmid pJB38-Δ*speG* was passaged through *E. coli* DC10B before electroporation
832 into *S. aureus* USA300 JE2 [91]. Deletion of *speG* was confirmed by PCR.
833 **Membrane permeabilization assay.** Fluorometric Disc3(5) membrane
834 permeabilization assays were performed as described in [55].
835 **Hemolysis Assay.** The hemolysis assay was performed using defibrinated sheep
836 blood (Thermo Fisher Scientific and Cedarlane) as previously described [92].
837 **Cell adhesion and cytotoxicity assays.** Madin-darby canine kidney (MDCK) cells
838 were cultured in DMEM with 10%(v/v) FBS and maintained according to the instructions. To
839 perform viability and adhesions assays, MDCK cells were split and seeded into Thermo
840 Scientific™ Nunc MicroWell 96-Well Optical-Bottom Plates (cat.165305) and grown
841 overnight to confluence (~$4x10^4$ per well). Adhered and confluent MDCK cells were then
842 washed 1x with sterile PBS and treated in serum-free DMEM with DMSO as a vehicle

843 control, OES2-017 at the USA300 MIC (20 μM), or OES1-01087at the MIC (1250 μM). A 2-
844 fold dilution series was performed for each compound down to 1/8 of the MIC. Treated
845 MDCK cells were incubated for 2h at 37℃ in a 5% CO_2 incubator. Before staining, and as
846 positive control to induce disruption of the MDCK monolayer individual, wells that were
847 previously left untreated were incubated with triton x-100 for 5 mins. Wells containing
848 MDCK cells were washed 1x with PBS and then incubated with TMR-wheat germ agglutin
849 (2 μg/mL) for 10 min in the cold. Cells were washed twice with PBs and then fixed with 4%
850 (v/v) PFA. To measure cell viability after 2h incubation with the compounds, the cells were
851 washed 1x with PBS and stained with Zombie Violet™ (Biolegend) according to the
852 manufacturer's instructions. The dye was used at a 1:500 dilution for 15 mins, and after
853 staining, the cells were washed twice with PBS and fixed as above. As a positive control,
854 prior zombie violet staining individual MDCK-containing wells were treated with 100% ice-
855 cold methanol for 3 mins prior to zombie violet staining. Fluorescence intensities for TMR-
856 WGA and Zombie Violet™ were measured using a Biotek Synergy H4 multimode plate
857 reader.
858
859 **Identification of homologous acetyltransferases.** *B. subtilis* BltD and PaiA protein
860 sequences were used as a query in a Position-Specific Iterative Basic Local Alignment
861 Search Tool (PSI-BLAST) search with results limited to records of *S. aureus* subsp. aureus
862 USA300_FPR3757. Results were filtered based on alignment scores (E value).
863 **Protein overexpression and purification.** *speG,* SAUSA300_2083,
864 SAUSA300_0441, and *paiA* were cloned into pET28a(+) and overexpressed under
865 conditions previously described [20]. cDNA of *SAT1* was codon-optimized, synthesized from,
866 and cloned into pET28a(+) (Bio Basic Canada). Lysis was achieved using a Branson
867 Sonifier 450 and the supernatant was isolated from the insoluble fraction by centrifugation
868 at 10 000 xg for 30 minutes at 4°C. His-tag batch purification was performed using His-
869 select nickel-affinity gel (Sigma-Aldrich). Purified proteins were detected on a 10%
870 acrylamide gel (Bio-Rad) by PageBlue staining solution (Fisher Scientific). Proteins were
871 quantified using the Bradford method with protein assay dye reagent concentrate (Bio-Rad),
872 following dialysis using SnakeSkin™ dialysis tubing (Fisher Scientific).
873
874 ***In vitro* SSAT enzymatic assays**

875 **Steady state kinetics.** Purified enzymes were used in spermine/spermidine *N*-
876 acetyltransferase (SSAT) colorimetric enzymatic assays as described previously [20,46], with
877 modifications. Briefly, 25 µL of enzyme solution (200 ng enzyme, 100 mM Tris-HCl, pH 7.5,
878 1 mM EDTA) were added to a 96 well plate then 50 µL of freshly prepared Ellman's reagent
879 [2 mM 5, 5'-dithio-bis-(2-nitrobenzoic acid) (DTNB) (Sigma Aldrich) 100 mM Tris-HCl, pH
880 7.5, 1 mM EDTA)] was added to each well. Finally, 25 µL of substrate solution was added to
881 begin the reaction. The substrate solution consisted of a final concentration of 1 mM acetyl-
882 CoA (Sigma Aldrich) with SpeG, $PaiA_{Sa}$, SAUSA300_2083, and SAUSA300_0441, and 0.25
883 mM acetyl-CoA with SAT1 in 100 mM Tris-HCl, pH 7.5, 1 mM EDTA with variable
884 concentrations of polyamines. Each reaction plate contained serial dilutions of Coenzyme A
885 (5-150 nmol) as a standard. Reactions were allowed to proceed at 37°C and $A_{412\ nm}$
886 readings were taken each minute for 45 min. Kinetic parameters were estimated by fitting
887 with the Michaelis-Menten equation or allosteric sigmoidal equation in Graphpad Prism 10.
888 **Enzymatic inhibition assays.** The colorimetric SSAT assay was performed where
889 25 µL of enzyme solution containing 200 ng enzyme, 100 mM Tris-HCl, pH 7.5, 1 mM
890 EDTA and a dilution series of inhibitor was added to a 96-well plate. The enzyme-inhibitor
891 solution was incubated at room temperature for 30 min before adding 50 µL Ellman's
892 reagent and 25 µL substrate solution to initiate the reaction. OES2-0017 and analogs in the
893 small-scale structure-activity relationship study were assayed with a substrate solution
894 including a fixed concentration of spermine ≈ K_m and 1 or 0.25 mM acetyl-CoA with SpeG
895 and SAT1, respectively. OES1-1087 inhibition was assayed with a substrate solution
896 including 1500 µM spermine and an AcCoA concentration at ~K_m. Substrate solution to
897 evaluate OES2-0017 inhibition of $PaiA_{Sa}$ contained a final concentration of 1 mM acetyl-
898 CoA and spermine at ~K_m. The reaction was monitored each minute at $A_{412\ nm}$ for 45
899 minutes. We evaluated the decrease in absorbance when the reaction was supplemented
900 with the inhibitors compared to a positive control containing only spermine and acetyl-CoA.
901 Data for IC_{50} plots were fit to a nonlinear regression inhibition model in Graphpad Prism 10
902 and K_i was estimated from equation 1 [93]. The colorimetric SSAT assay was also performed
903 in a 96-well plate where enzyme activity was monitored in the presence of the respective
904 inhibitor across 8 concentrations of substrate and data were fit to a competitive inhibition
905 model in Graphpad Prism 10.
906 Equation 1: $IC_{50} = K_i\ (1+ \frac{[S]}{Km})$

907

908 **Macrophage infections.** RAW-264.7 cells were seeded ($1x10^6$ cells/mL) in RPMI
909 (Sigma Aldrich) supplemented with 10% fetal bovine serum (Fisher Scientific), 1 mM
910 HEPES (Thermofisher), and 100X MEM non-essential amino acids solution (Thermofisher)
911 in 24-well plates 2 days prior to infection and incubated at 37°C and 5% CO_2. *S.*
912 Typhimurium 14028s wild-type and *speG*::Cm were grown in appropriate selection for 16 h
913 at 37°C. Bacteria were subcultured in LB with no antibiotics until late log phase. The OD_{600}
914 was normalized and cells washed with fresh media, 10 μL of washed cells were added to 1
915 mL of supplemented RPMI and 50 μL of the diluted bacteria was added to each well. Plates
916 were centrifuged at 1000 rpm for 1 minute and incubated at 37°C, 5% CO_2 for 10 minutes to
917 complete infection. Media were replaced (1 mL/well) at ten minutes post-infection, with
918 RPMI supplemented with 100 μg/mL gentamicin for 30 minutes to kill extracellular bacteria.
919 After 30 minutes, fresh RPMI media supplemented with 10 μg/mL gentamicin with and
920 without 10 μM OES2-0017 were added. Plates were then incubated for 4 hours. The pre-
921 infection group was treated with 10 μM OES2-0017 30 minutes prior to infection with *S.*
922 Typhimurium. Cells were lysed by washing twice with 1 mL 1X PBS and then adding 1 mL
923 1% PBS-Triton for 5 minutes per well. Lysed cells were diluted and plated on LB agar and
924 incubated at 37°C for 16 hours. Cells were lysed and plated at time 0, 4 hours post-
925 infection, and 15 hours post-infection.

926 **Phylogenetic analysis.** Protein BLAST analysis was used to identify proteins with
927 homology to *S. aureus* SpeG. Sequences were downloaded in FASTA format and a multiple
928 sequence alignment was generated using MUSCLE. A phylogenetic tree was constructed
929 using a neighbor joining method using MEGA11 and visualized using iTOL.

930 **Docking and 3D Protein Homology.** The ligand protein docking was done using
931 SwissDock (https://www.swissdock.ch/) and the docking results were visualized using
932 UCSF Chimera-1.17.3 (https://www.cgl.ucsf.edu/chimera/). The interacting amino acid
933 residues of the target protein were further illustrated by BIOVIA Discovery Studio Visualizer
934 (https://www.3ds.com/products/biovia/discovery-studio/visualization). 3D homology and
935 alignments between different proteins were performed by PyMOL 3.0
936 (https://www.pymol.org/).

937

938 **Acknowledgements**

This work was supported by Natural Sciences and Engineering Research Council of Canada discovery grant (RGPIN-2022-04239 and DGECR-2022- 00206), a Saskatchewan Health Research Foundation establishment grant (6115), a Canadian Institutes of Health Research grant (202403PPE- 522800), and start-up funds from the Faculty of Science at the University of Regina to OME. OME holds a Canada Research Chair in Chemogenomics and Antimicrobial Research (CRC-2019-00115). PBM and JW were supported by a Canadian Institutes of Health Research Canada Graduate Scholarship—Master's (CGS-M) award. PBM was also supported by the Verna Martin Memorial Scholarship. WE holds a Canada Research Chair in Microbiome Research (CRC-00249). WE is funded by Crohn's & Colitis Canada, Natural Sciences and Engineering Research Council of Canada, Major Innovation Fund, Antimicrobial Resistance - One Health Consortium, and Striving for Pandemic Preparedness - The Alberta Research Consortium (SPP-ARC). Work in the DEH laboratory was funded by an operating grant (PJT-183848) from the Canadian Institutes of Health Research.

954 **References**

955 1. Murray, C.J. et al. Global burden of bacterial antimicrobial resistance in 2019: a
956 systematic analysis. *Lancet* **399**, 629-655 (2022).
957 2. WHO. *Prioritization of pathogens to guide discovery, research and development of new*
958 *antibiotics for drug-resistant bacterial infections, including tuberculosis*, (World Health
959 Organization, Geneva, 2017).
960 3. Taylor, T.A. & Unakal, C.G. *Staphylococcus aureus Infection*, (StatPearls Publishing,
961 Treasure Island (FL), 2023).
962 4. Nichol, K.A. et al. Characterization of MRSA in Canada from 2007 to 2016. *J Antimicrob*
963 *Chemother* **74**, iv55-iv63 (2019).
964 5. Diekema, D.J. et al. Continued emergence of USA300 methicillin-resistant
965 *Staphylococcus aureus* in the United States: results from a nationwide surveillance
966 study. *Infect Control Hosp Epidemiol* **35**, 285-92 (2014).
967 6. Beyer, P. & Paulin, S. The Antibacterial Research and Development Pipeline Needs
968 Urgent Solutions. *ACS Infect Dis* **6**, 1289-1291 (2020).
969 7. Miethke, M. et al. Towards the sustainable discovery and development of new
970 antibiotics. *Nat Rev Chem* **5**, 726-749 (2021).
971 8. CLSI. *Methods for Dilution Antimicrobial Susceptibility Tests for Bacteria that Grow*
972 *Aerobically Approved Standard—Tenth Edition M07-A10*, (2012).
973 9. El-Halfawy, O.M. & Valvano, M.A. Non-genetic mechanisms communicating antibiotic
974 resistance: rethinking strategies for antimicrobial drug design. *Expert Opin Drug Discov*
975 **7**, 923-33 (2012).
976 10. Moulding, P.B. & El-Halfawy, O.M. Chemical-mediated virulence: the effects of host
977 chemicals on microbial virulence and potential new antivirulence strategies. *Can J*
978 *Microbiol* (2024).
979 11. Tabor, C.W. & Tabor, H. Polyamines. *Annu Rev Biochem* **53**, 749-90 (1984).
980 12. Yao, X. & Lu, C.D. Functional characterization of the potRABCD operon for spermine
981 and spermidine uptake and regulation in Staphylococcus aureus. *Curr Microbiol* **69**, 75-
982 81 (2014).
983 13. Gazdar, A.F., Stull, H.B., Kilton, L.J. & Bachrach, U. Increased ornithine decarboxylase
984 activity in murine sarcoma virus infected cells. *Nature* **262**, 696-8 (1976).
985 14. Thurlow, L.R. et al. Functional modularity of the arginine catabolic mobile element
986 contributes to the success of USA300 methicillin-resistant *Staphylococcus aureus*. *Cell*
987 *Host Microbe* **13**, 100-7 (2013).
988 15. Watanabe, S., Kusama-Eguchi, K., Kobayashi, H. & Igarashi, K. Estimation of polyamine
989 binding to macromolecules and ATP in bovine lymphocytes and rat liver. *J Biol Chem*
990 **266**, 20803-9 (1991).
991 16. Igarashi, K. & Kashiwagi, K. Modulation of cellular function by polyamines. *Int J Biochem*
992 *Cell Biol* **42**, 39-51 (2010).
993 17. Moinard, C., Cynober, L. & de Bandt, J.P. Polyamines: metabolism and implications in
994 human diseases. *Clin Nutr* **24**, 184-97 (2005).
995 18. Zhang, M., Wang, H. & Tracey, K.J. Regulation of macrophage activation and
996 inflammation by spermine: a new chapter in an old story. *Crit Care Med* **28**, N60-6
997 (2000).
998 19. Joshi, G.S., Spontak, J.S., Klapper, D.G. & Richardson, A.R. Arginine catabolic mobile
999 element encoded *speG* abrogates the unique hypersensitivity of *Staphylococcus aureus*
1000 to exogenous polyamines. *Mol Microbiol* **82**, 9-20 (2011).
1001 20. Li, B. et al. Polyamine-independent growth and biofilm formation, and functional
1002 spermidine/spermine N-acetyltransferases in *Staphylococcus aureus* and *Enterococcus*
1003 *faecalis*. *Mol Microbiol* **111**, 159-175 (2019).

1004 21. Seravalli, J., Portugal, F. & Putrescine Detected in Strains of *Staphylococcus aureus*.
1005 *Pathogens* **12**, 881 (2023).
1006 22. Diep, B.A. et al. The arginine catabolic mobile element and staphylococcal chromosomal
1007 cassette mec linkage: convergence of virulence and resistance in the USA300 clone of
1008 methicillin-resistant *Staphylococcus aureus*. *J Infect Dis* **197**, 1523-30 (2008).
1009 23. Planet, P.J. et al. Emergence of the epidemic methicillin-resistant *Staphylococcus*
1010 *aureus* strain USA300 coincides with horizontal transfer of the arginine catabolic mobile
1011 element and *speG*-mediated adaptations for survival on skin. *MBio* **4**, e00889-13 (2013).
1012 24. Fang, S.B. et al. *speG* Is Required for Intracellular Replication of *Salmonella* in Various
1013 Human Cells and Affects Its Polyamine Metabolism and Global Transcriptomes. *Front*
1014 *Microbiol* **8**(2017).
1015 25. Martini, C. et al. The polyamine *N*-acetyltransferase-like enzyme PmvE plays a role in
1016 the virulence of *Enterococcus faecalis*. *Infect Immun* **83**, 364-71 (2015).
1017 26. Yao, X. & Lu, C.D. A PBP 2 mutant devoid of the transpeptidase domain abolishes
1018 spermine-beta-lactam synergy in *Staphylococcus aureus* Mu50. *Antimicrob Agents*
1019 *Chemother* **56**, 83-91 (2012).
1020 27. Kwon, D.H. & Lu, C.D. Polyamines induce resistance to cationic peptide,
1021 aminoglycoside, and quinolone antibiotics in *Pseudomonas aeruginosa* PAO1.
1022 *Antimicrob Agents Chemother* **50**, 1615-22 (2006).
1023 28. Kwon, D.H. & Lu, C.D. Polyamine effects on antibiotic susceptibility in bacteria.
1024 *Antimicrob Agents Chemother* **51**, 2070-7 (2007).
1025 29. Li, J., Beuerman, R. & Verma, C.S. Mechanism of polyamine induced colistin resistance
1026 through electrostatic networks on bacterial outer membranes. *Biochim Biophys Acta*
1027 *Biomembr* **1862**, 183297 (2020).
1028 30. Adams, J.M.E., Moulding, P.B. & El-Halfawy, O.M. Polyamine-Mediated Sensitization of
1029 *Klebsiella pneumoniae* to Macrolides through a Dual Mode of Action. *ACS Infect Dis* **10**,
1030 2183-2195 (2024).
1031 31. McGinnis, M.W. et al. Spermidine regulates *Vibrio cholerae* biofilm formation via
1032 transport and signaling pathways. *FEMS Microbiol Lett* **299**, 166-74 (2009).
1033 32. Liu, Z., Hossain, S.S., Morales Moreira, Z. & Haney, C.H. Putrescine and Its Metabolic
1034 Precursor Arginine Promote Biofilm and c-di-GMP Synthesis in *Pseudomonas*
1035 *aeruginosa*. *J Bacteriol* **204**, e0029721 (2022).
1036 33. Patel, C.N. et al. Polyamines are essential for the formation of plague biofilm. *J Bacteriol*
1037 **188**, 2355-63 (2006).
1038 34. Nasrallah, G.K. et al. *Legionella pneumophila* requires polyamines for optimal
1039 intracellular growth. *J Bacteriol* **193**, 4346-60 (2011).
1040 35. Shah, P., Nanduri, B., Swiatlo, E., Ma, Y. & Pendarvis, K. Polyamine biosynthesis and
1041 transport mechanisms are crucial for fitness and pathogenesis of *Streptococcus*
1042 *pneumoniae*. *Microbiology (Reading)* **157**, 504-515 (2011).
1043 36. Johnson, L., Mulcahy, H., Kanevets, U., Shi, Y. & Lewenza, S. Surface-localized
1044 spermidine protects the *Pseudomonas aeruginosa* outer membrane from antibiotic
1045 treatment and oxidative stress. *J Bacteriol* **194**, 813-26 (2012).
1046 37. Dickey, S.W., Cheung, G.Y.C. & Otto, M. Different drugs for bad bugs: antivirulence
1047 strategies in the age of antibiotic resistance. *Nat Rev Drug Discov* **16**, 457-471 (2017).
1048 38. Dhanda, G., Acharya, Y. & Haldar, J. Antibiotic Adjuvants: A Versatile Approach to
1049 Combat Antibiotic Resistance. *ACS Omega* **8**, 10757-10783 (2023).
1050 39. El-Halfawy, O.M. & Valvano, M.A. Chemical communication of antibiotic resistance by a
1051 highly resistant subpopulation of bacterial cells. *PLOS One* **8**, e68874 (2013).
1052 40. Kallio, A. & McCann, P.P. Difluoromethylornithine irreversibly inactivates ornithine
1053 decarboxylase of *Pseudomonas aeruginosa*, but does not inhibit the enzymes of
1054 *Escherichia coli*. *Biochem J* **200**, 69-75 (1981).

1055 41. Mattila, T., Honkanen-Buzalski, T. & Poso, H. Reversible inhibition of bacterial growth
1056 after specific inhibition of spermidine synthase by dicyclohexylamine. *Biochem J* **223**,
1057 823-30 (1984).
1058 42. Fey, P.D. et al. A genetic resource for rapid and comprehensive phenotype screening of
1059 nonessential *Staphylococcus aureus* genes. *mBio* **4**, e00537-12 (2013).
1060 43. Maki, H., McCallum, N., Bischoff, M., Wada, A. & Berger-Bachi, B. tcaA inactivation
1061 increases glycopeptide resistance in *Staphylococcus aureus*. *Antimicrob Agents*
1062 *Chemother* **48**, 1953-9 (2004).
1063 44. Tsai, M. et al. *Staphylococcus aureus* requires cardiolipin for survival under conditions of
1064 high salinity. *BMC Microbiol* **11**, 13 (2011).
1065 45. Beasley, F.C., Cheung, J. & Heinrichs, D.E. Mutation of L-2,3-diaminopropionic acid
1066 synthase genes blocks staphyloferrin B synthesis in *Staphylococcus aureus*. *BMC*
1067 *Microbiol* **11**, 199 (2011).
1068 46. Lin, H.J., Lien, Y.C. & Hsu, C.H. A high-throughput colorimetric assay to characterize the
1069 enzyme kinetic and cellular activity of spermidine/spermine N1-acetyltransferase 1. *Anal*
1070 *Biochem* **407**, 226-32 (2010).
1071 47. Tsimbalyuk, S. et al. Structural and Kinetic Characterization of the SpeG
1072 Spermidine/Spermine N-acetyltransferase from Methicillin-Resistant Staphylococcus
1073 aureus USA300. *Cells* **12**(2023).
1074 48. Zhu, J., Dhimitruka, I. & Pei, D. 5-(2-Aminoethyl)dithio-2-nitrobenzoate as a more base-
1075 stable alternative to Ellman's reagent. *Org Lett* **6**, 3809-12 (2004).
1076 49. Filippova, E.V. et al. A novel polyamine allosteric site of SpeG from Vibrio cholerae is
1077 revealed by its dodecameric structure. *J Mol Biol* **427**, 1316-1334 (2015).
1078 50. Tsimbalyuk, S., Shornikov, A., Thi Bich Le, V., Kuhn, M.L. & Forwood, J.K. SpeG
1079 polyamine acetyltransferase enzyme from Bacillus thuringiensis forms a dodecameric
1080 structure and exhibits high catalytic efficiency. *J Struct Biol* **210**, 107506 (2020).
1081 51. Le, V.T.B. et al. The Vibrio cholerae SpeG Spermidine/Spermine N-Acetyltransferase
1082 Allosteric Loop and beta6-beta7 Structural Elements Are Critical for Kinetic Activity.
1083 *Front Mol Biosci* **8**, 645768 (2021).
1084 52. Filippova, E.V. et al. Substrate-Induced Allosteric Change in the Quaternary Structure of
1085 the Spermidine N-Acetyltransferase SpeG. *J Mol Biol* **427**, 3538-3553 (2015).
1086 53. Woolridge, D.P., Martinez, J.D., Stringer, D.E. & Gerner, E.W. Characterization of a
1087 novel spermidine/spermine acetyltransferase, BltD, from *Bacillus subtilis*. *Biochem J* **340**
1088 **(Pt 3)**, 753-8 (1999).
1089 54. Forouhar, F. et al. Structural and functional evidence for Bacillus subtilis PaiA as a novel
1090 N1-spermidine/spermine acetyltransferase. *J Biol Chem* **280**, 40328-36 (2005).
1091 55. Farha, M.A., Verschoor, C.P., Bowdish, D. & Brown, E.D. Collapsing the proton motive
1092 force to identify synergistic combinations against *Staphylococcus aureus*. *Chem Biol* **20**,
1093 1168-78 (2013).
1094 56. Yasuda, K., Ohmizo, C. & Katsu, T. Mode of action of novel polyamines increasing the
1095 permeability of bacterial outer membrane. *Int J Antimicrob Agents* **24**, 67-71 (2004).
1096 57. Armalyte, J. et al. A polyamine acetyltransferase regulates the motility and biofilm
1097 formation of Acinetobacter baumannii. *Nat Commun* **14**, 3531 (2023).
1098 58. Matsui, I., Kamei, M., Otani, S., Morisawa, S. & Pegg, A.E. Occurrence and induction of
1099 spermidine-*N*1-acetyltransferase in *Escherichia coli*. *Biochem Biophys Res Commun*
1100 **106**, 1155-60 (1982).
1101 59. Hu, L.I. et al. The spermidine acetyltransferase SpeG regulates transcription of the small
1102 RNA *rprA*. *PLoS One* **13**, e0207563 (2018).
1103 60. *WHO Bacterial Priority Pathogens List, 2024: bacterial pathogens of public health*
1104 *importance to guide research, development and strategies to prevent and control*
1105 *antimicrobial resistance*, (World Health Organization, Geneva, 2024).

1106 61. Dever, T.E. & Ivanov, I.P. Roles of polyamines in translation. *J Biol Chem* **293**, 18719-
1107 18729 (2018).
1108 62. Igarashi, K. & Kashiwagi, K. Polyamines: mysterious modulators of cellular functions.
1109 *Biochem Biophys Res Commun* **271**, 559-64 (2000).
1110 63. Liu, W.T. et al. Emerging resistance mechanisms for 4 types of common anti-MRSA
1111 antibiotics in *Staphylococcus aureus*: A comprehensive review. *Microb Pathog* **156**,
1112 104915 (2021).
1113 64. Ma, H. et al. Adjunctive rifampin for the treatment of *Staphylococcus aureus* bacteremia
1114 with deep infections: A meta-analysis. *PLoS One* **15**, e0230383 (2020).
1115 65. Choo, E.J. & Chambers, H.F. Treatment of Methicillin-Resistant *Staphylococcus aureus*
1116 Bacteremia. *Infect Chemother* **48**, 267-273 (2016).
1117 66. Bewley, M.C. et al. Structures of wild-type and mutant human spermidine/spermine N1-
1118 acetyltransferase, a potential therapeutic drug target. *Proc Natl Acad Sci U S A* **103**,
1119 2063-8 (2006).
1120 67. Hegde, S.S., Chandler, J., Vetting, M.W., Yu, M. & Blanchard, J.S. Mechanistic and
1121 structural analysis of human spermidine/spermine N1-acetyltransferase. *Biochemistry*
1122 **46**, 7187-95 (2007).
1123 68. Zahedi, K. et al. Spermidine/spermine-N1-acetyltransferase ablation protects against
1124 liver and kidney ischemia-reperfusion injury in mice. *Am J Physiol Gastrointest Liver*
1125 *Physiol* **296**, G899-909 (2009).
1126 69. Xu, J. et al. Inhibition of SAT1 alleviates chondrocyte inflammation and ferroptosis by
1127 repressing ALOX15 expression and activating the Nrf2 pathway. *Bone Joint Res* **13**,
1128 110-123 (2024).
1129 70. Jin, Z., Xu, H., Sun, X., Yan, B. & Wang, L. Targeting SAT1 prevents osteoporosis
1130 through promoting osteoclast apoptosis. *Biomed Pharmacother* **175**, 116732 (2024).
1131 71. Zahedi, K., Barone, S. & Soleimani, M. Polyamine Catabolism in Acute Kidney Injury. *Int*
1132 *J Mol Sci* **20**(2019).
1133 72. Russell, D.H. Increased polyamine concentrations in the urine of human cancer patients.
1134 *Nat New Biol* **233**, 144-5 (1971).
1135 73. Maksymiuk, A.W. et al. Spermidine/spermine N1-acetyltransferase-1 as a diagnostic
1136 biomarker in human cancer. *Future Sci OA* **4**, FSO345 (2018).
1137 74. Wallace, H.M. & Fraser, A.V. Inhibitors of polyamine metabolism: review article. *Amino*
1138 *Acids* **26**, 353-65 (2004).
1139 75. Egorov, O.S. et al. Structure and biological action of analogs and derivatives of biogenic
1140 polyamines. *Fine Chemical Technologies* **16**, 287-306 (2021).
1141 76. Boncher, T., Bi, X., Varghese, S., Casero, R.A., Jr. & Woster, P.M. Polyamine-based
1142 analogues as biochemical probes and potential therapeutics. *Biochem Soc Trans* **35**,
1143 356-63 (2007).
1144 77. Blanchet, M., Borselli, D. & Brunel, J.M. Polyamine derivatives: a revival of an old
1145 neglected scaffold to fight resistant Gram-negative bacteria? *Future Med Chem* **8**, 963-
1146 73 (2016).
1147 78. Chen, D. et al. alpha,omega-Diacyl-Substituted Analogues of Natural and Unnatural
1148 Polyamines: Identification of Potent Bactericides That Selectively Target Bacterial
1149 Membranes. *Int J Mol Sci* **24**(2023).
1150 79. Douglas, E.J.A. et al. Antibacterial activity of novel linear polyamines against
1151 Staphylococcus aureus. *Front Microbiol* **13**, 948343 (2022).
1152 80. Libby, P.R. & Porter, C.W. Inhibition of enzymes of polyamine back-conversion by
1153 pentamidine and berenil. *Biochem Pharmacol* **44**, 830-2 (1992).
1154 81. Karvonen, E., Kauppinen, L., Partanen, T. & Poso, H. Irreversible inhibition of
1155 putrescine-stimulated S-adenosyl-L-methionine decarboxylase by berenil and
1156 pentamidine. *Biochem J* **231**, 165-9 (1985).

1157 82. Homeida, A.M., El Amin, E.A., Adam, S.E. & Mahmoud, M.M. Toxicity of diminazene
1158 aceturate (Berenil) to camels. *J Comp Pathol* **91**, 355-60 (1981).
1159 83. Elamin, E.A., Homeida, A.M., Adam, S.E. & Mahmoud, M.M. The efficacy of berenil
1160 (diminazene aceturate) against *Trypanosoma evansi* infection in mice. *J Vet Pharmacol*
1161 *Ther* **5**, 259-65 (1982).
1162 84. Passaglia, P. et al. Diminazene aceturate attenuates systemic inflammation via
1163 microbiota gut-5-HT brain-spleen sympathetic axis in male mice. *Brain Behav Immun*
1164 **119**, 105-119 (2024).
1165 85. Coutinho, D.C.O. et al. Diminazene Aceturate, an angiotensin converting enzyme 2
1166 (ACE2) activator, promotes cardioprotection in ischemia/reperfusion-induced cardiac
1167 injury. *Peptides* **151**, 170746 (2022).
1168 86. da Silva Oliveira, G.L. & de Freitas, R.M. Diminazene aceturate--An antiparasitic drug of
1169 antiquity: Advances in pharmacology & therapeutics. *Pharmacol Res* **102**, 138-57
1170 (2015).
1171 87. Isoproterenol. Isoproterenol. (Medscape - https://reference.medscape.com/drug/isuprel-
1172 isoproterenol-342438#91, 2024).
1173 88. Farha, M.A. & Brown, E.D. Drug repurposing for antimicrobial discovery. *Nat Microbiol* **4**,
1174 565-577 (2019).
1175 89. Peters, J.M. et al. A comprehensive, CRISPR-based functional analysis of essential
1176 genes in bacteria. *Cell* **165**, 1493-1506 (2016).
1177 90. Bose, J.L., Fey, P.D. & Bayles, K.W. Genetic tools to enhance the study of gene function
1178 and regulation in *Staphylococcus aureus*. *Appl Environ Microbiol* **79**, 2218-24 (2013).
1179 91. Grosser, M.R. & Richardson, A.R. Method for Preparation and Electroporation of *S.*
1180 *aureus* and *S. epidermidis*. *Methods Mol Biol* **1373**, 51-7 (2016).
1181 92. Barker, W.T., Chandler, C.E., Melander, R.J., Ernst, R.K. & Melander, C. Tryptamine
1182 derivatives disarm colistin resistance in polymyxin-resistant gram-negative bacteria.
1183 *Bioorg Med Chem* **27**, 1776-1788 (2019).
1184 93. Cheng, Y. & Prusoff, W.H. Relationship between the inhibition constant (K1) and the
1185 concentration of inhibitor which causes 50 per cent inhibition (I50) of an enzymatic
1186 reaction. *Biochem Pharmacol* **22**, 3099-108 (1973).

1187